

Chapter – 4 Results and Discussion

CHAPTER 4

RESULTS AND DISCUSSION

This chapter is divided into three parts for avoiding the complexity of the discussion. Part-I deals with polymer (polyamide) silica nanocomposite film, part-II deals with polymer (polypropylene) silica nanocomposite filament and part-III deals with polymer (polyester) silica nanocomposite fabric. The prepared polymer silica nanocomposite textiles were analyzed by standard techniques for evaluating changes in structural and mechanical behavior and compared with respective pure material.

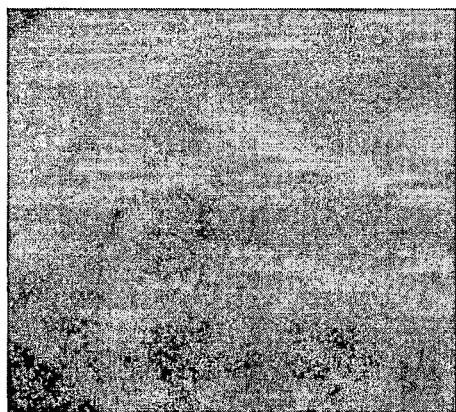
4.1 PART – I: POLYMER SILICA NANOCOMPOSITE FILM

Silica nanoparticles at 0.1%, 0.3%, 0.5%, 0.7% & 1.0% concentration level were mixed with polyamide chips in formic acid as solvent with constant stirring at 250 rpm. The mixture was heated at 60 °C for 1 hr., finally the polymer/nanocomposite mixture were poured in flat glass dish and allowed the solvent to evaporate, which resulted in terms of distribution of SiO₂ nano particles throughout the film as shown in figure 4.1. The effect on the structural and mechanical properties has been presented in this section. The nomenclature used during the discussion for the samples prepared is given in following table 4.1.

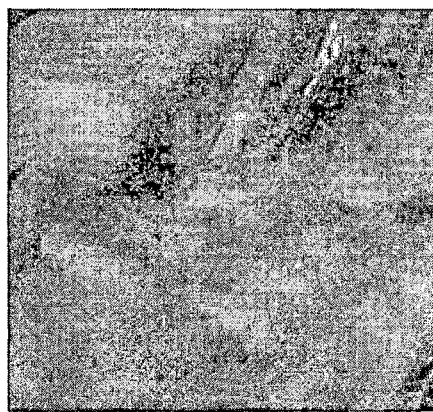
Table 4.1 Nomenclature of Polyamide silica nanocomposite films

| Sr. No. | Sample | Silica (gm) |
|---------|--------|---|
| 1 | PA | Pure Polyamide film |
| 2 | NPA1 | Polyamide film with 0.1% addition of SiO ₂ |
| 3 | NPA2 | Polyamide film with 0.3% addition of SiO ₂ |
| 4 | NPA3 | Polyamide film with 0.5% addition of SiO ₂ |
| 5 | NPA4 | Polyamide film with 0.7% addition of SiO ₂ |
| 6 | NPA5 | Polyamide film with 1.0% addition of SiO ₂ |

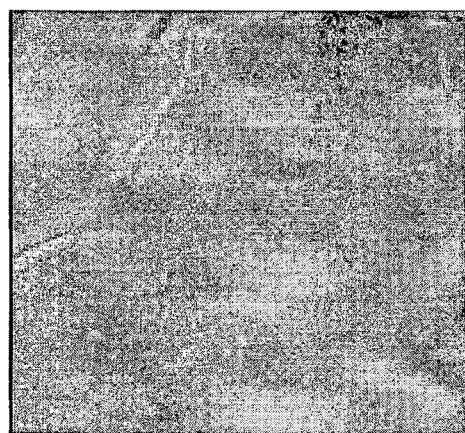
PA: polyamide, NPA: Nano silica loaded polyamide



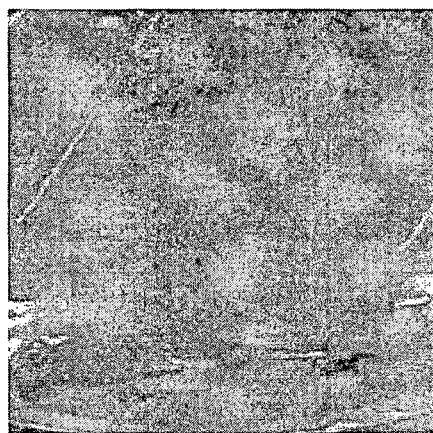
a) Pure Polyamide film



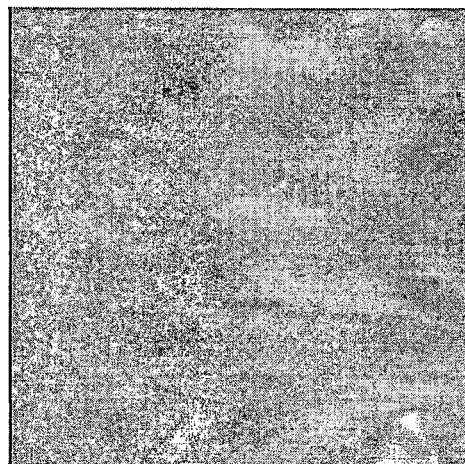
b) PA+0.1% nano silica



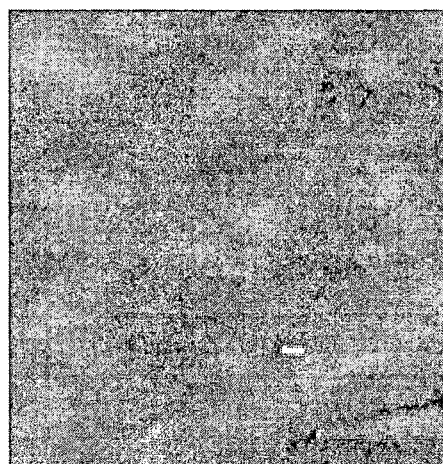
c) PA+0.3% nano silica



d) PA+0.5% nano silica



e) PA+0.7% nano silica



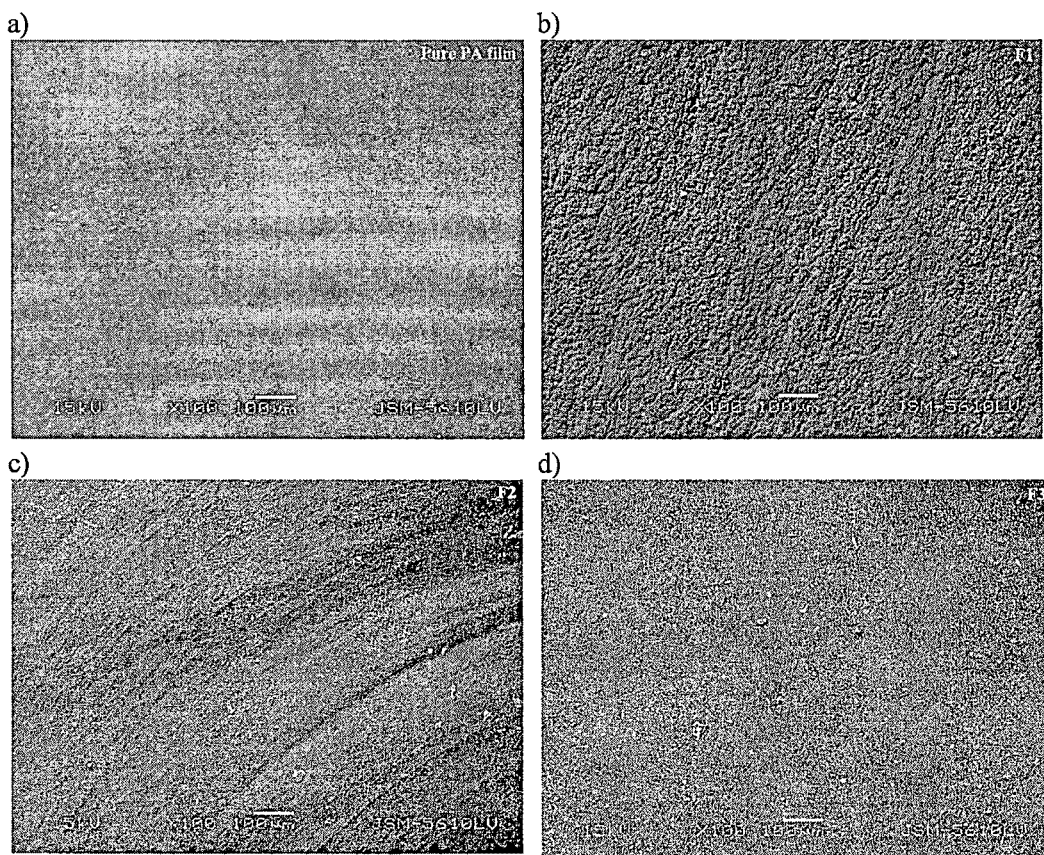
f) PA+1.0% nano silica

Figure 4.1 Polyamide untreated (a) and treated (b to f) films

4.1.1 STRUCTURAL ANALYSIS

4.1.1.1 Surface morphological analysis through SEM

Figure 4.2 a) shows the SEM micrograph of pure polyamide film. Figure 4.2 (b to f) shows the nanocomposite films with 0.1%, 0.3%, 0.5%, 0.7% and 1.0% concentration of silica nano particles in polyamide matrix prepared from dissolution mixing method. In figure 4.2 b), c) and d) the uniform distribution of nano particles is observed. Figure 4.2 e) shows the some non-uniform distribution of SiO_2 nano particles. Figure 4.2 f) shows the agglomeration of silica nanoparticles and deterioration of film in terms of its continuity, the holes have been observed in the film.



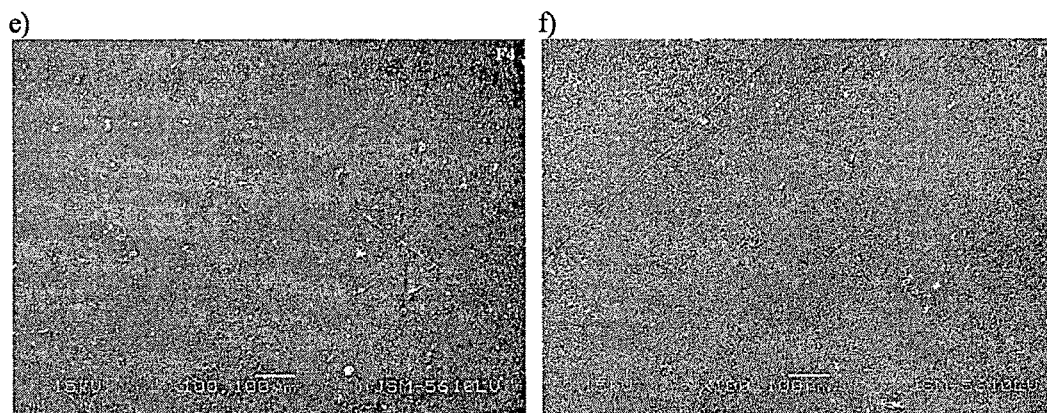
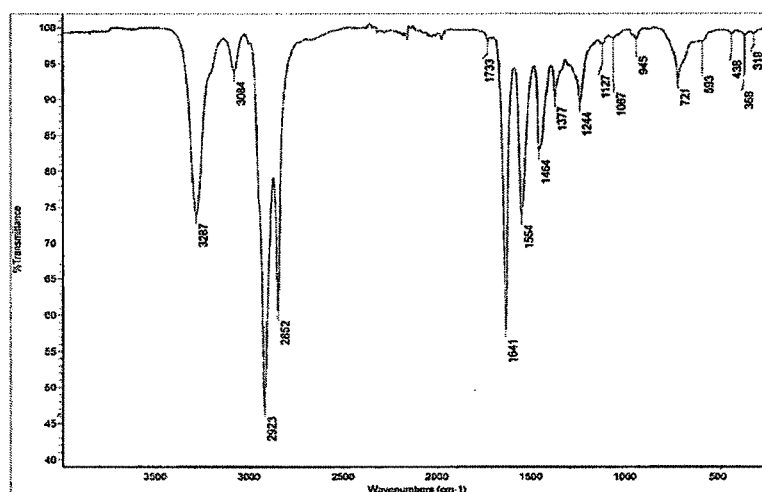


Figure 4.2 SEM micrographs of pure polyamide and polyamide/SiO₂ nanocomposite films, a) pure polyamide film, b) polyamide+0.1% nano SiO₂, c) polyamide+0.3% nano SiO₂, d) polyamide+0.5% nano SiO₂, e) polyamide+0.7% nano SiO₂, f) polyamide+ 1.0% nano SiO₂.

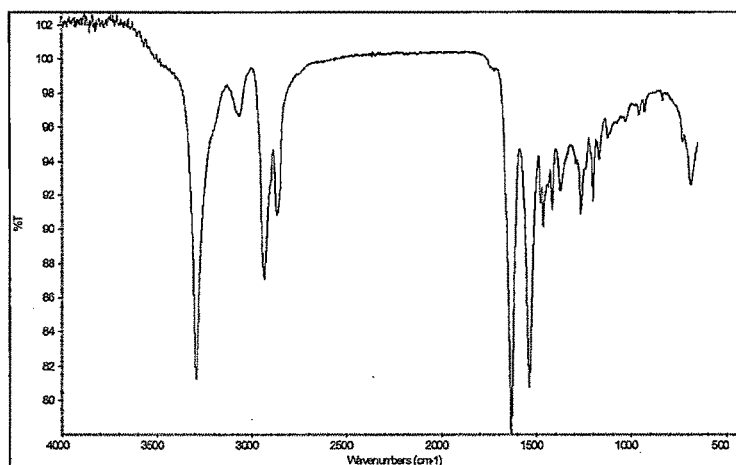
4.1.1.2 FTIR spectral analysis



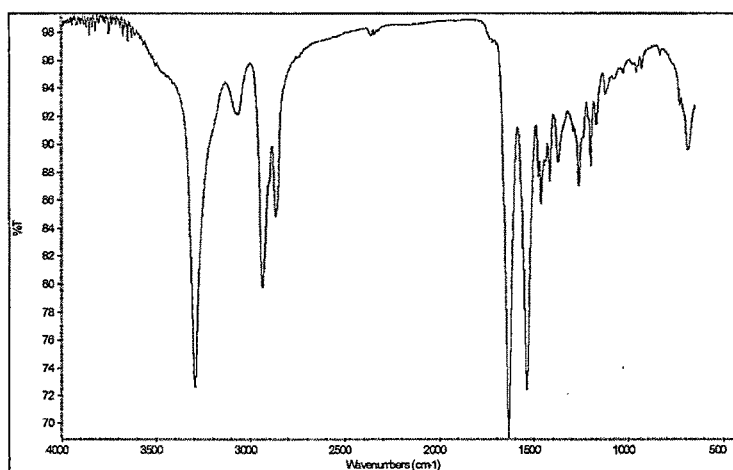
a) Pure Polyamide film

The chemical compositions of the pure polyamide and polyamide/silica nanocomposite films were evaluated using FTIR Spectroscopy. Table 4.2 and figure 4.3 (a) represents the IR characterization absorption peak of pure polyamide film, from which it can be seen that the peaks associated were hydrogen bonded N-H stretching at 3287 cm⁻¹ [140], C-H stretching at 3084 cm⁻¹, asymmetric stretching vibrations of C-H [141] at 2923 cm⁻¹, Symmetric stretching vibrations of C-H [141]

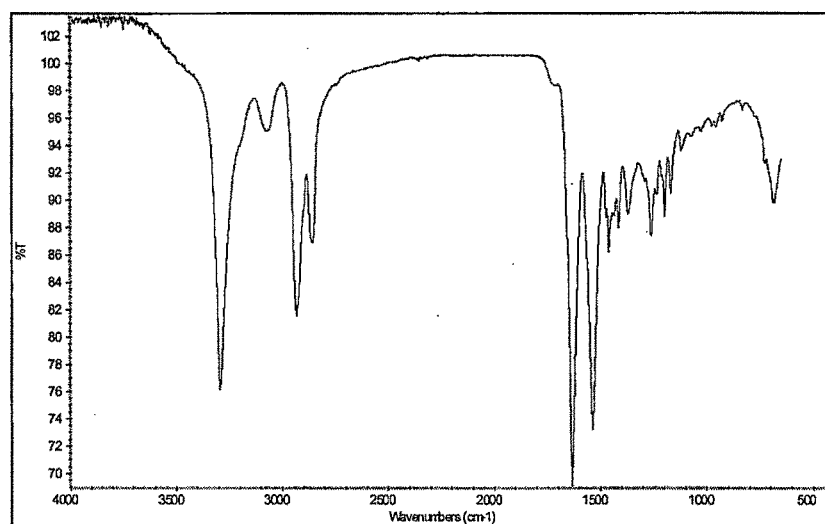
bonds at 2852 cm^{-1} , peak 1733 cm^{-1} [142] corresponding to the carboxyl groups, $\text{C}=\text{O}$ [140] stretching at 1641 cm^{-1} , N-H bending at 1554 cm^{-1} , the presence of these modes suggests presence of a polyamide., CH_2 symmetric bending vibration-scissoring type at 1464 cm^{-1} , CH_3 bending at 1377 cm^{-1} , inplane C-H bending at 1244 cm^{-1} , C-H stretching at 1127 cm^{-1} , O-H stretching at 1067 cm^{-1} , C-H stretching at 945 cm^{-1} and CH_2 bending vibrations-rocking type observed at 721 cm^{-1} .



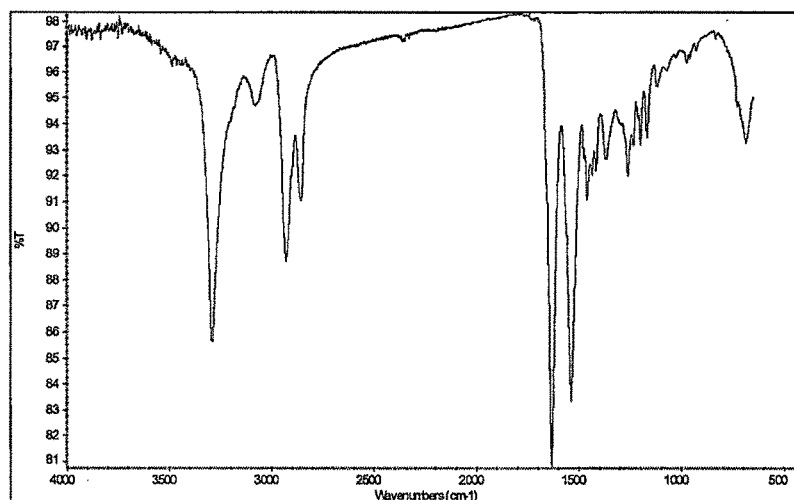
b) Polyamide and 0.1% SiO₂ film



c) Polyamide and 0.3% SiO₂ film



d) Polyamide and 0.5% SiO₂ film



e) Polyamide and 0.7% SiO₂ film

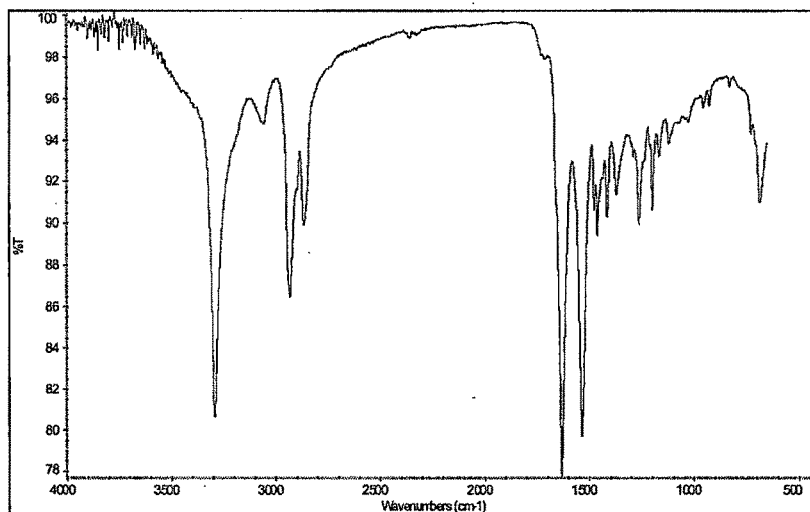
f) Polyamide and 1.0% SiO₂ film

Figure 4.3 IR absorption peaks of pure polyamide (a) and polyamide/Silica nanocomposite films (b to f).

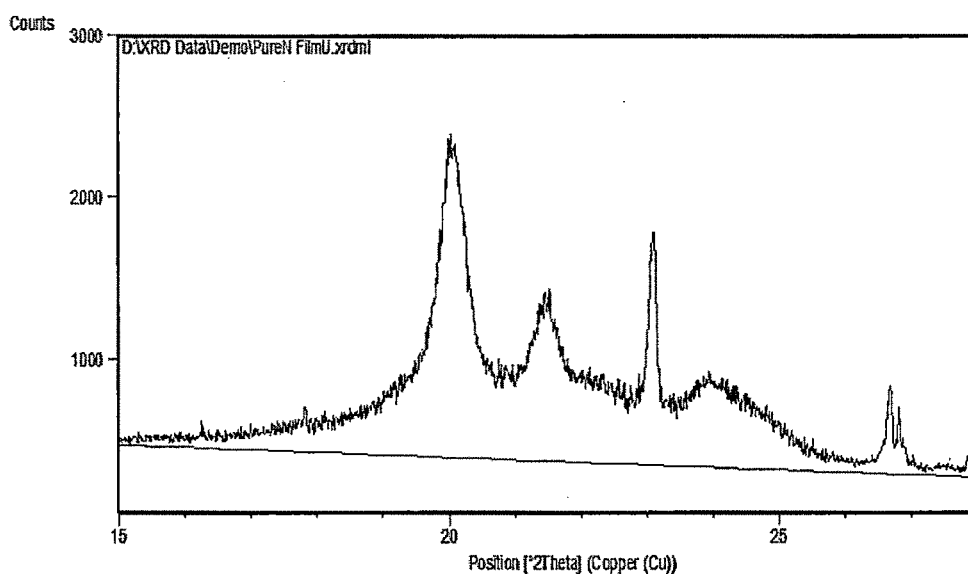
Peaks shown by pure polyamide film are identical in all nanocomposite films as shown in figure 4.3 (b to f), additionally the nanocomposite films showed the peaks of silica around 840 cm⁻¹ corresponds to Si-O [143] bending vibration, absorption peak belonging to the Si-OH [141] bond appears at 920 cm⁻¹, band around 1098 cm⁻¹ correspond to asymmetric stretching vibration of Si-O-Si [144] band. Due to addition of silica nano particles in polyamide in different concentrations, the FTIR peaks showed the increased stretching vibrations of O-H in the range of 3600 to 3900 cm⁻¹ in all spectrographs of nanocomposite films, also C-O stretches observed at 1160 cm⁻¹ and 1210 cm⁻¹, C-H bend at 1410 cm⁻¹ as shown in figure 4.3 (b to f).

Table 4.2 FTIR characterization peaks of pure polyamide and polyamide / Silica nanocomposite films

| Groups | Wavenumber (cm ⁻¹) | | | | | |
|---|--------------------------------|--------------|--------------|--------------|--------------|--------------|
| | PA | NPA1 | NPA2 | NPA3 | NPA4 | NPA5 |
| CH ₂ bending vibrations-rocking type | 721 | 721 | 721 | 721 | 721 | 721 |
| C-H bending | 945 | 945 | 945 | 945 | 945 | 945 |
| O-H stretching | 1067 | 1067 | 1067 | 1067 | 1067 | 1067 |
| C-H stretching | 1127 | 1127 | 1127 | 1127 | 1127 | 1127 |
| Inplane CH bending | 1244 | 1244 | 1244 | 1244 | 1244 | 1244 |
| CH ₃ bending | 1377 | 1377 | 1377 | 1377 | 1377 | 1377 |
| CH ₂ symmetric bending vibration-scissoring type | 1464 | 1464 | 1464 | 1464 | 1464 | 1464 |
| N-H bending | 1554 | 1554 | 1554 | 1554 | 1554 | 1554 |
| C=O stretching | 1641 | 1641 | 1641 | 1641 | 1641 | 1641 |
| Carboxyl group | 1733 | 1733 | 1733 | 1733 | 1733 | 1733 |
| Symmetric vibrations of C-H | 2852 | 2852 | 2852 | 2852 | 2852 | 2852 |
| Asymmetric vibrations of C-H | 2923 | 2923 | 2923 | 2923 | 2923 | 2923 |
| C-H stretching | 3084 | 3084 | 3084 | 3084 | 3084 | 3084 |
| N-H stretching | 3287 | 3287 | 3287 | 3287 | 3287 | 3287 |
| Si-O bending vibration | - | 840 | 840 | 840 | 840 | 840 |
| Absorption peak belonging to the Si-OH bond | - | 920 | 920 | 920 | 920 | 920 |
| Asymmetric stretching vibration of Si-O-Si band | - | 1098 | 1098 | 1098 | 1098 | 1098 |
| C-O stretches | - | 1160 | 1160 | 1160 | 1160 | 1160 |
| C-O stretches | - | 1210 | 1210 | 1210 | 1210 | 1210 |
| C-H bend | - | 1410 | 1410 | 1410 | 1410 | 1410 |
| Stretching vibrations of O-H | - | 3600 to 3900 | 3600 to 3900 | 3600 to 3900 | 3600 to 3900 | 3600 to 3900 |

4.1.1.3 X-ray diffraction Analysis

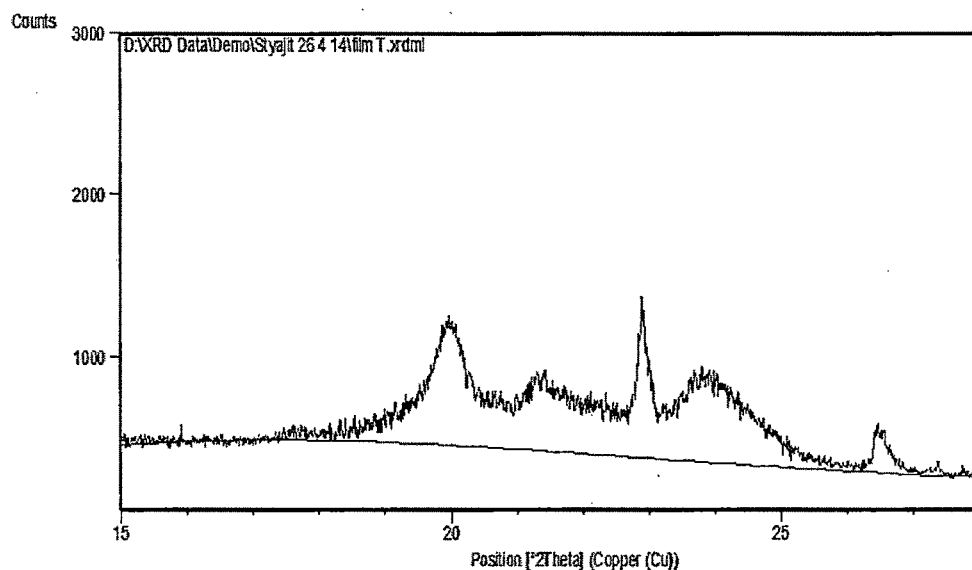
The X-ray diffraction patterns were taken on X'pert Pro PANalytical x-ray diffractometer. The XRD of both the fabrics was done within the 2θ range of 10° to 30° at the scan speed of 3° per minute at 25°C temperature, using Cu-K_α radiation of wavelength 1.5406\AA . The diffraction profiles were obtained for individual samples. The XRD patterns are given in figure 4.4 and 4.5 for PA and NPA4 samples i.e. pure polyamide film and 0.7% nano silica in polyamide film respectively. The combined XRD patterns of both the samples are shown in figure 4.6.



| Pos. [2θ] | Height [cts] | d-spacing [\AA] | Area [cts $\cdot 2\theta$] | Rel. Int. [%] |
|--------------------|--------------|----------------------------|-----------------------------|---------------|
| 20.047 | 1662 | 4.42562 | 1277.34 | 100 |
| 21.520 | 659 | 4.12788 | 763.61 | 39.643 |
| 23.082 | 1114 | 3.85021 | 214.55 | 67.021 |
| 23.99 | 316 | 3.70665 | 314.68 | 19.025 |
| 26.669 | 396 | 3.33987 | 70.64 | 23.805 |

Figure 4.4 XRD pattern of pure polyamide film (PA)

XRD pattern of PA sample shows sharp and broad features with reasonably high intensity. Four prominent peaks are observed. The pattern exhibits a certain degree of amorphicity. However, the characteristic peaks are well defined and quite intense. The peak at 2θ value of 20.047° has the highest intensity followed by 23.082° , 21.510° & 26.669° and these peaks are of polyamide polymer [145].



| Pos. [$^{\circ}2\theta$] | Height [cts] | d-spacing [\AA] | Area [cts $\times^{\circ}2\theta$] | Rel. Int. [%] |
|----------------------------|--------------|----------------------------|-------------------------------------|---------------|
| 19.952 | 671 | 4.44653 | 774.26 | 99.68 |
| 21.54 | 357 | 4.12165 | 703.96 | 53.06 |
| 22.90 | 672 | 3.88029 | 162.01 | 100 |
| 23.95 | 500 | 3.71303 | 1032.55 | 74.44 |
| 26.505 | 286 | 3.36024 | 67.60 | 42.42 |

Figure 4.5 XRD pattern of polyamide silica nanocomposite film (NPA4)

The incorporation of silica nano particles lead to the development of some kind of force which drifts the atomic planes, such that the d-value increases. From the figure it can be seen that the crystallinity of the treated sample is of lower order compared to the untreated samples. However, the SEM micrographs show the incorporation of silica nano particles within the film. These particles might disperse the x-rays incident on the film. This may be reason for decrease in the peak intensity of the treated film and not the crystallinity of the film itself. Due to addition of nano silica in polyamide, the peak intensity is reduced from 2400, 1428, 1750, 1000 and 850 to 1250, 900, 1380, 920 and 580 respectively. This may be due to diffraction or deviation of x-rays by the nano silica particles. Hence, the number of x-rays reaching the detector might be less. The d-values for the observed diffraction peak of silica is in close agreement with those reported for corresponding standard samples as reported in JCPDS data file no. 84-0384. One of the peaks corresponding to d-value of 4.4414 \AA is in complete agreement.

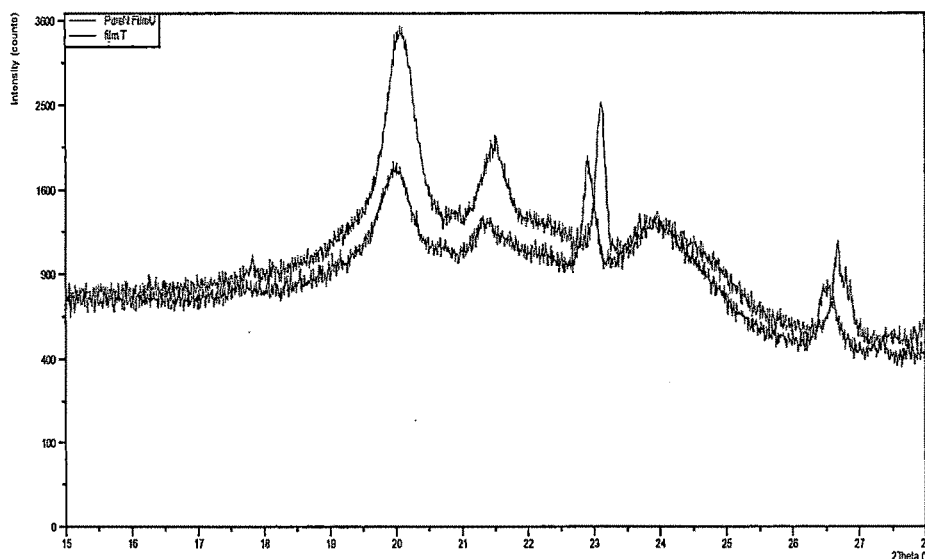


Figure 4.5 Combined XRD patterns of PA and NPA4 samples

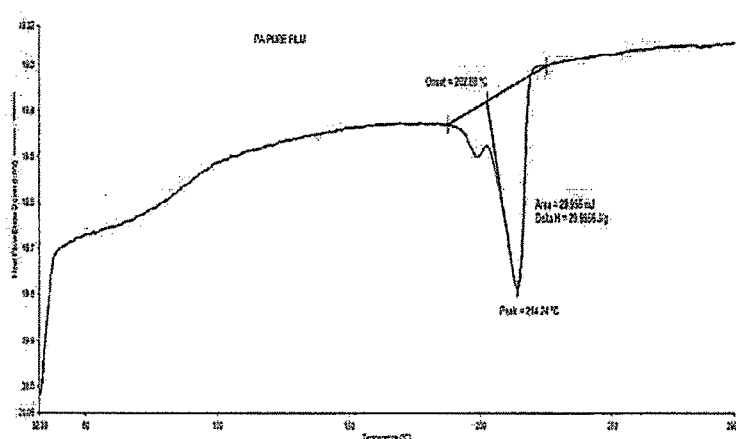
4.1.1.4 Thermal analysis

The effect on thermal property due to incorporation of silica nano particles in polyamide film is studied through differential scanning calorimetry (DSC). The silica nano particles were added in different proportions as 0.1%, 0.3%, 0.5%, 0.7% and 1.0% on weight bases. The thermal behavior of pure and nanocomposite film is shown in figure 4.7 and the results are given in table 4.3.

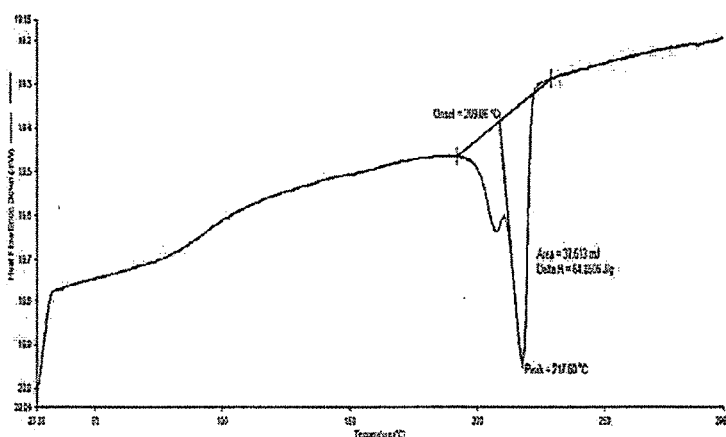
Table 4.3 Enthalpy (ΔH) of pure polyamide and polyamide/silica nanocomposite film

| Sample | % Concentration of nano SiO ₂ | Melting Temperature (°C) | Enthalpy (ΔH) (J/g) | % Change in Enthalpy (ΔH) | Crystallinity % |
|--------|--|--------------------------------|-------------------------------------|--|--------------------|
| PA | 0.0 | 214.24 | 30.00 | 0 | 13.04 |
| NPA1 | 0.1 | 217.8 | 64.85 | 116.17 | 28.21 |
| NPA2 | 0.3 | 215.64 | 52.89 | 76.30 | 23.05 |
| NPA3 | 0.5 | 218.31 | 49.55 | 65.17 | 21.64 |
| NPA4 | 0.7 | 215.14 | 46.58 | 55.27 | 20.39 |
| NPA5 | 1.0 | 209.31 | 22.87 | -23.77 | 10.04 |

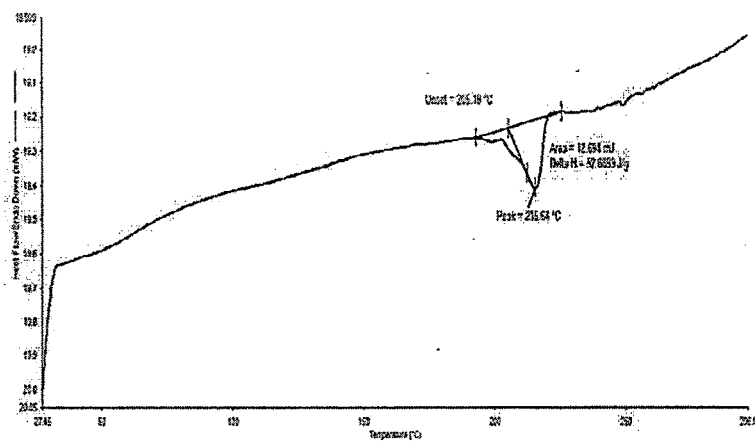
Figure 4.7 (a) shows the differential scanning calorimetry (DSC) curve of pure polyamide film. Here the pure polyamide film sample was heated at 10°C/min rate upto 300°C, in which it shows the melting temperature of the film as 214.24°C and the total heat required to melt i.e. enthalpy (ΔH) is 30 J/g, the % crystallinity calculated on the bases of enthalpy is 13.04%. DSC curves for polyamide sometime exhibits three or two or one peak. In this experimental work pure polyamide film exhibited two peaks; the reason may be the polyamide has different forms of lamellar thickness like α , γ , and δ forms [146].



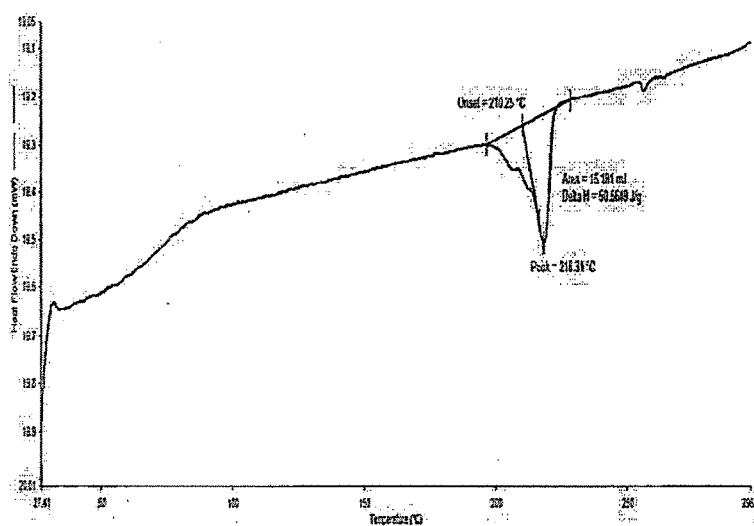
a) DSC curve of Pure Polyamide film



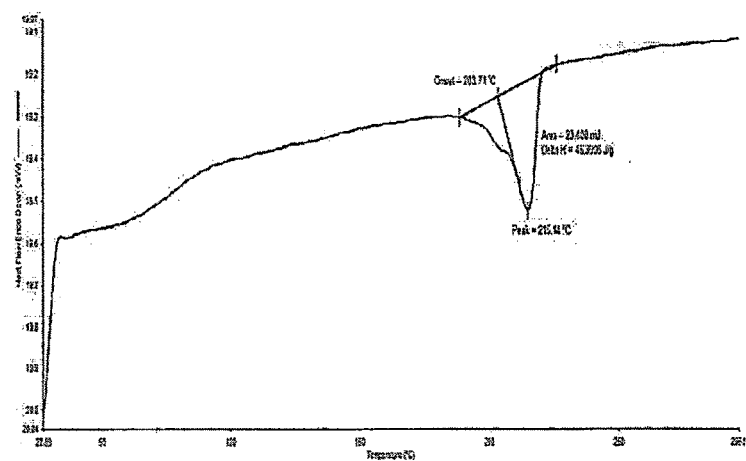
b) DSC curve of Polyamide and 0.1% SiO₂ film



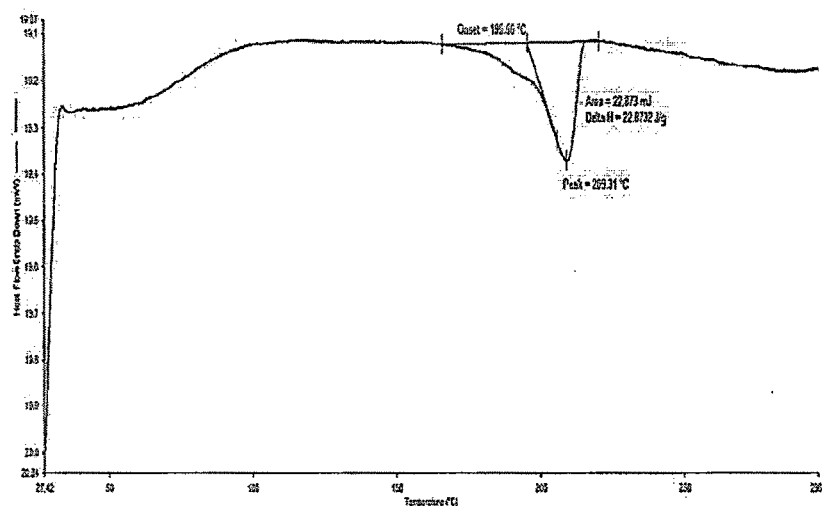
c) DSC curve of Polyamide and 0.3% SiO₂ film



d) DSC curve of Polyamide and 0.5% SiO₂ film



e) DSC curve of Polyamide and 0.7% SiO₂ film

f) DSC curve of Polyamide and 1.0% SiO₂ film**Figure 4.7** DSC curves of pure polyamide (a) and polyamide silica nanocomposite films (b to f)

The NPA1 i.e. 0.1% concentration of nano silica sample also exhibited two similar peaks like pure polyamide sample, but NPA2 and NPA3 samples exhibited three peaks, this means that the change is taking place in lamellar thickness of polyamide structure due to addition of nano silica by 0.3% and 0.5% concentrations. Further addition of nano material by 0.7% in polyamide i.e. NPA4 sample exhibits two peaks and in sample NPA5 i.e. 1%, these peaks are getting merged into one peak. This means that with further increase in nano silica concentrations i.e. 0.7% and 1%, there is again change in structure take place.

Figure 4.7 (b to f) show the DSC curves of nanocomposite films of polyamide and SiO₂ nano particles at different concentration levels like 0.1%, 0.3%, 0.5%, 0.7% and 1.0%. The melting temperature, enthalpy and % crystallinity of all films is given in table 4.3. The melting temperature of pure polyamide film is 214.24°C and there is no significant effect on melting temperature due to addition of silica nano particles, except the 1.0% silica nanocomposite polyamide film, where there is significant drop in melting temperature i.e. 209.31°C. This reduction in melting temperature may be due to degradation of the film i.e. holes are observed in SEM micrographs of the film (figure 4.2 (f)). This has also reflected in less enthalpy required to melt this film as

compare to pure polyamide film. The results show that there is a significant difference in ΔH between virgin PA and PA/silica nanocomposite films. At higher concentration of silica nano particles in PA matrix, indicating that silica in agglomerate form was not able to alter the thermal behavior of PA. On the other hand, lower concentration of nano silica in dissolution mixed PA/silica nanocomposite has a higher ΔH value than virgin PA. In this case, silica size is reduced into a nanoscopic level, hence inducing better thermal stability of the film [147]. In PA/silica nanocomposite films two melting peaks observed, but these two peaks are getting merged into one as the concentration of nano silica particles is increasing, which is clearly seen in NPA5 sample.

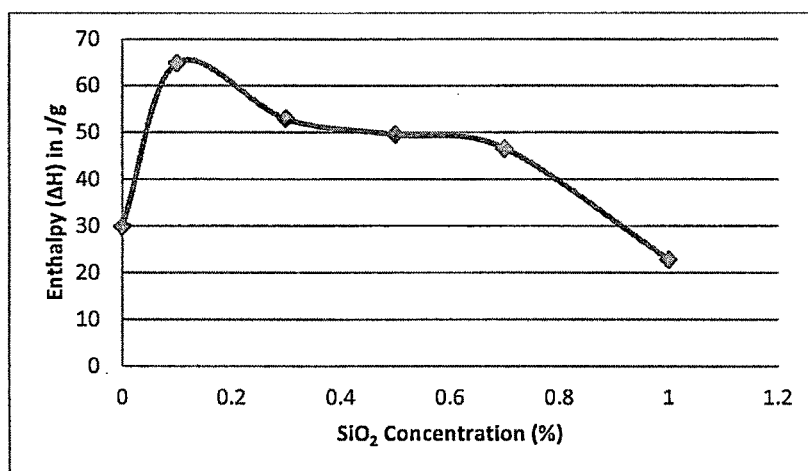


Figure 4.8 Percentage change in Enthalpy (ΔH) of polyamide/silica nanocomposite film

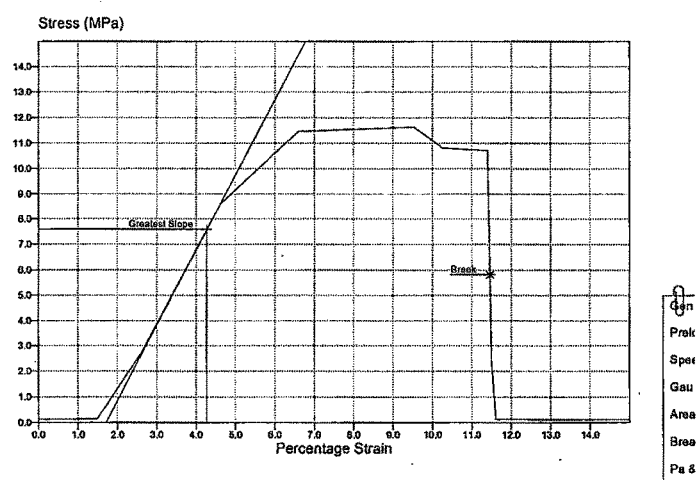
The percentage change in enthalpy of silica treated nanocomposite film is found more than virgin polyamide by 116.17%, 76.30%, 65.17% and 55.27% for 0.1%, 0.3%, 0.5% and 0.7% concentrations respectively. The same trend is seen in case of crystallinity of film. In less concentration of nano silica would be giving better stability to the film as compare to higher concentration of silica nano particles. Overall the enthalpy required to melt the nanocomposite films is higher than pure polyamide film. But in case of 1% concentration of nano silica, the enthalpy required to melt the film has found less than pure film i.e. 22.87 J/g. This may be due to the high concentration of nano silica particles which may cause agglomeration of nano particles and not allowing to form continuous structure of polyamide and damaged the film, which can be clearly seen from the SEM micrographs.

4.1.2 MECHANICAL PROPERTIES

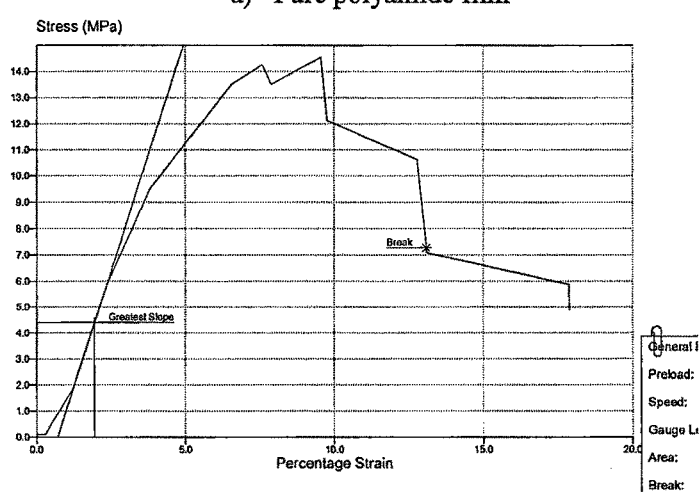
The effect on mechanical properties i.e. tensile, young's modulus and work of rupture due to incorporation of silica nanoparticles in polyamide film is studied here. The silica nanoparticles were added in different proportions as 0.1, 0.3, 0.5, 0.7 and 1.0 percentage on weight bases.

4.1.2.1 Tensile property

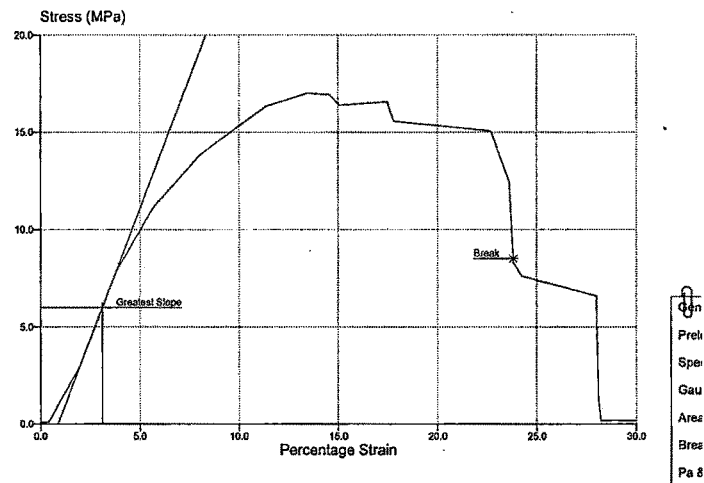
The tensile test was performed on Llyod LRX tensile testing machine and the stress strain curve of various samples tested are summarized in table 4.4 and shown in figure 4.9 below.



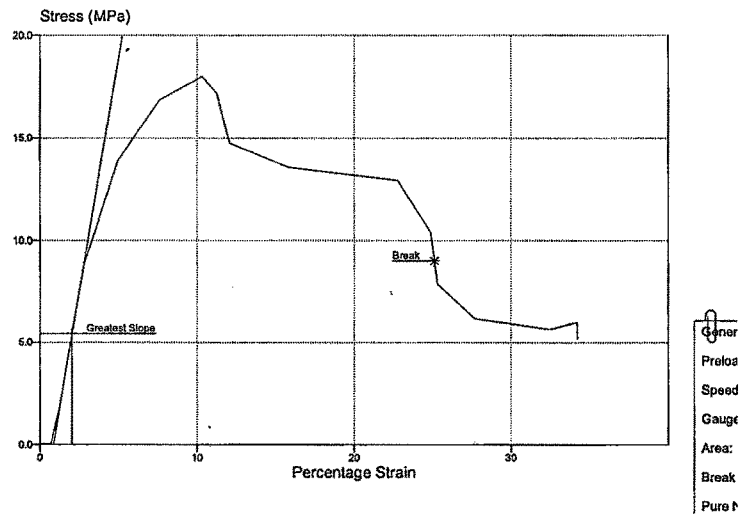
a) Pure polyamide film



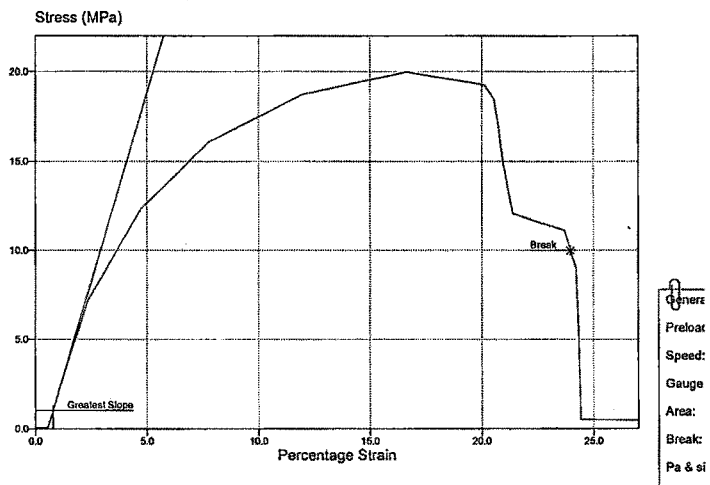
b) Polyamide and 0.1% SiO₂ film



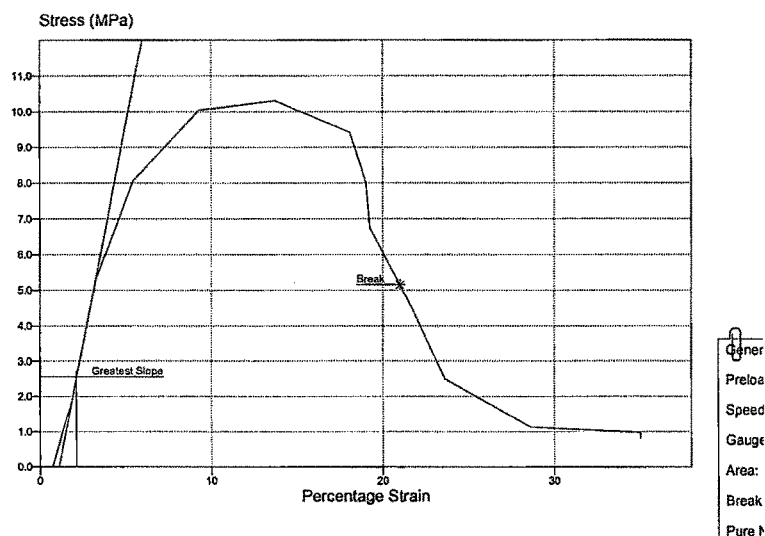
c) Polyamide and 0.3% SiO₂ film



d) Polyamide and 0.5% SiO₂ film



e) Polyamide and 0.7% SiO₂ film



f) Polyamide and 1.0% SiO₂ film

Figure 4.9 Stress strain behavior of pure polyamide (a) and polyamide/Silica nanocomposite films (b to f).

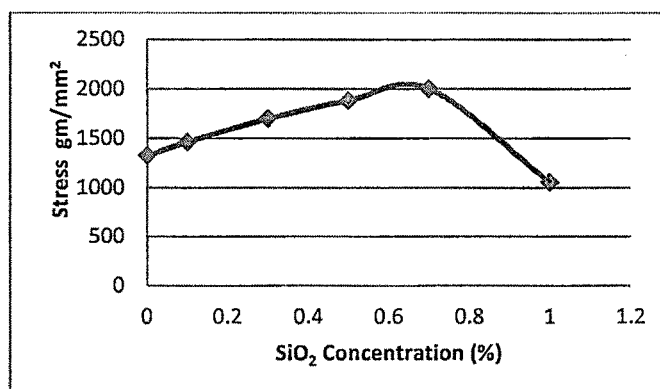
The results given in table 4.4 and stress strain curves in figure 4.9 reveals that the obtained nanocomposite film exhibits an increase in specific strength with an increase in percent silica loading (silica loading of 0.1 wt % to 0.7 wt % respectively), it may be due to the phenomenon of reinforcement effect at nanoscopic level. However, the composite film at higher concentration of nano silica exhibits the erratic trend of tensile strength value due to the phase separation problem arising from particles' agglomeration. Also SEM result is showing the deterioration of film for 1.0 % concentration of SiO₂ nano particles in terms of its continuity, as film becomes brittle and breaks easily i.e. holes have been observed in the film in SEM micrographs figure 4.2 (f). Good mechanical property results are obtained at 0.7% loading of nano silica polyamide film and then it shows decrease in mechanical property. Such changes in mechanical properties i.e. tensile strength, elongation and stiffness was also observed by Hagenmueller, et al., 2003; Poncharal, et al., 1999; Stegmaier, 2006; Kalarikkal, Sankar, and Ifju, 2006 [12-15].

Table 4.4 Effect of SiO₂ nano silica on tensile property of nanocomposite films

| Sample | % Concentra tion of nano SiO ₂ | Thickness in Mm | Maximum Load in gf | Elongation % | Area = Width x thickness in mm ² | Specific strength in gm/mm ² |
|--------|--|--------------------|--------------------------|-----------------|--|--|
| PA | 0.0 | 0.0427 | 1418.4 | 12.02 | 1.0694 | 1326.35 |
| NPA1 | 0.1 | 0.03 | 1098.8 | 9.52 | 0.75 | 1465.07 |
| NPA2 | 0.3 | 0.0819 | 3484.3 | 13.41 | 2.0486 | 1700.82 |
| NPA3 | 0.5 | 0.0444 | 2102.8 | 14.37 | 1.115 | 1885.92 |
| NPA4 | 0.7 | 0.0491 | 2463.6 | 16.39 | 1.2291 | 2004.39 |
| NPA5 | 1.0 | 0.0472 | 1244.2 | 14.48 | 1.1805 | 1053.96 |

Width=25.4 mm, Gauge Length=20 mm

The stress (specific strength) is found increasing by 10.55%, 28.15%, 42.11% and 51.04% for 0.1%, 0.3%, 0.5% and 0.7% concentration of nano silica in polyamide film respectively as compare to pure polyamide film. This may be due to increase in concentration and uniform distribution of nano particles in polymer matrix, which can be seen from the SEM micrographs. Above 0.7% concentration, it is observed that the stress property decreases by 20.62% for 1% concentration of nano silica in polyamide film as compare to pure polyamide film. This may be due to agglomeration of nano silica in polymer matrix, which is making the film brittle and so it gets broken easily and thus reducing the stress of polyamide silica nano composite film, which has also caused damage to the film. Small holes on the surface of the film can be seen in SEM micrographs figure 4.2 (f).

**Figure 4.10** Effect of nano silica on stress property of film

4.1.2.2 Young's modulus and work of rupture

The table 4.5 and figure 4.11 and 4.12 show the young's modulus and stiffness properties of virgin polyamide film and nano silica loaded polyamide films, the young's modulus is directly proportional to the stiffness property. Here the young's modulus is calculated on the bases of Meredith's method. The virgin polyamide film is showing lower young's modulus and stiffness i.e. 136.25 gf/mm² and 11.10 KN/m respectively than the polyamide silica loaded nanocomposite films i.e. 173.68 & 26.21, 161.15 & 30.54, 250.11 & 30.89 and 230.39 & 31.69 respectively for 0.1%, 0.3%, 0.5% and 0.7% concentration of nano silica particles in polyamide film, except 1% concentration film i.e. 78.05 & 16.59. The young's modulus is found increased with addition of silica nano particles and also there is further overall rise in young's modulus with increase in percentage loading of silica nano particles i.e. upto 0.7% concentration and above this i.e. at 1% concentration of silica nano particles, the drop in young's modulus is observed which is 66.12% from the value of young's modulus of 0.7% concentration sample. Similarly, the stiffness property is also increasing with the increase in concentration of nano silica in polyamide i.e. upto 0.7% and thereafter at 1% concentration of nano silica the stiffness is decreased by 47.65% from the maximum value.

Table 4.5 Effect of nano silica on young's modulus, stiffness and work of rupture

| Sample | Concentration of nano SiO ₂ (%) | Young's Modulus (gf/mm ²) | Stiffness (KN/m) | Work of rupture at maximum load (gf.mm) |
|--------|--|---|---------------------|---|
| PA | 0.0 | 136.25 | 11.10 | 1023.0 |
| NPA1 | 0.1 | 173.68 | 26.21 | 2708.0 |
| NPA2 | 0.3 | 161.15 | 30.54 | 6695.1 |
| NPA3 | 0.5 | 250.11 | 30.89 | 3343.0 |
| NPA4 | 0.7 | 230.39 | 31.69 | 7228.0 |
| NPA5 | 1.0 | 78.05 | 16.59 | 2778.9 |

It is observed that up to 0.7% of filler loading, the composite film gives better results compared to pure polyamide film, but as the loading of silica increased above 0.7%, the film becomes brittle and breaks easily, which also can be seen from the SEM

microphotograph in figure 4.2 (f). Overall the stiffness of the nano silica loaded polyamide films are showing rise except 1% concentration. The 1.0% nano silica loaded polyamide film would not be allowing the material to become compact due to agglomeration of the nano particles and becoming more brittle, which would be hindering the development of compact structure, which is also supported by the reduction in enthalpy required to melt the 1% concentration nano silica polyamide nanocomposite film in DSC as shown in figure 4.7 (f).

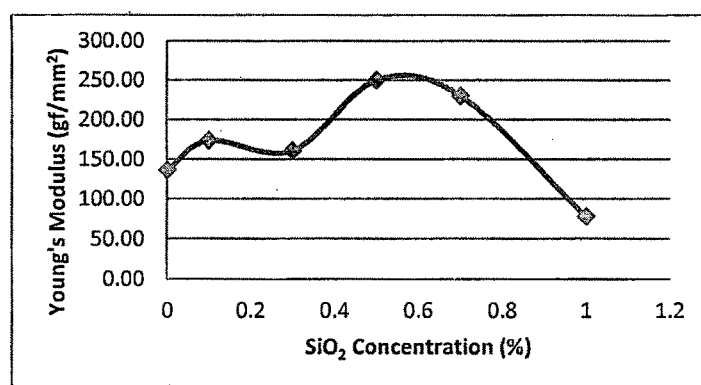


Figure 4.11 Effect of nano silica on young's modulus of treated and untreated polyamide films

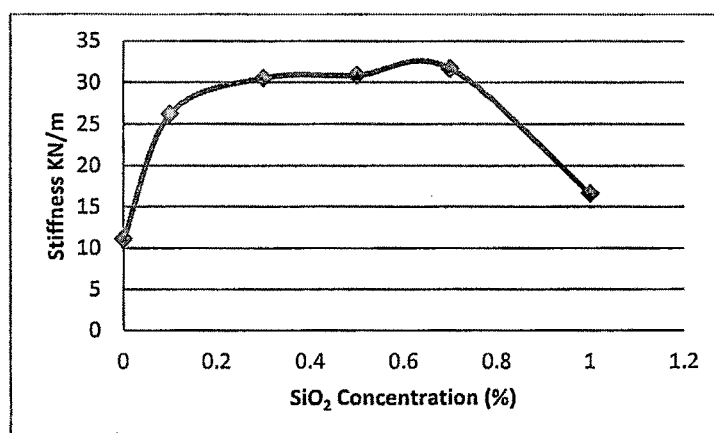


Figure 4.12 Effect of nano silica on stiffness of treated and untreated polyamide films

The work of rupture is a measure of the “toughness” of the material. It is the energy or work required to break the specimen. The area under the load-elongation curve represents the work done in stretching the material to breaking point. The work of

rupture value indicates the resistance of the material to sudden shock [148]. Table 4.5 and figure 4.13 show the work at maximum load of virgin polyamide film and nano silica loaded polyamide films. The work required to break the virgin polyamide film is 1023 gf.mm which is less as compare to nano silica treated polyamide nanocomposite films. Overall, the work of rupture is found increased with addition of silica nano particles and also there is further rise with increase in loading of silica nano particles i.e. 2708, 6695.1, 3343 and 7228 gf.mm, except 0.5% loading sample has shown the drop in work of rupture but overall the work is higher than pure polyamide film. Further, the 1% concentration sample is also showing the drop in work of rupture i.e. 2778.9 gf.mm, but here also the work is higher than the virgin polyamide film. The other properties of this sample, like enthalpy, young's modulus and stiffness are also showing the drop, and the reason could be the agglomeration induced brittleness in film, which can also be seen from the SEM micrographs. Here also, it is observed that up to 0.7% of filler loading, the composite film gives better results compared to pure polyamide film, but as the loading of silica increased above 0.7%, the film becomes brittle and breaks easily, it may be due to agglomeration of nano particles, which also can be seen from the SEM microphotograph in figure 4.2 (f). Overall the work of rupture of the nano silica loaded polyamide films are showing rise as compare to virgin film, except 1% concentration. The 1.0% nano silica loaded polyamide film would not be allowing the material to become compact due to agglomeration of the nano particles and becoming more brittle, which would be hindering the development of compact structure.

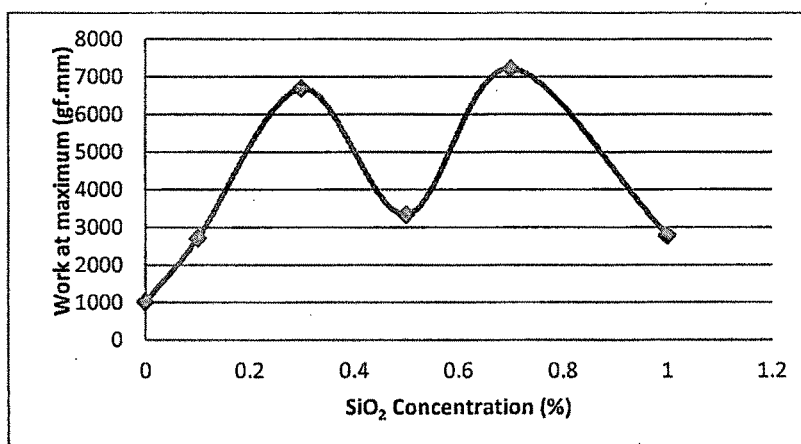


Figure 4.13 Effect of nano silica on work at maximum load of treated and untreated polyamide films

4.2 PART – II: POLYMER SILICA NANOCOMPOSITE FILAMENT

In this part, the basic polymer was changed from polyamide to polypropylene in filament form, and the concentration of silica nano particles is kept same as polyamide film. The filaments with different proportions of silica nanoparticles were prepared using pilot melt spinning plant. The evaluation of prepared polymer silica nanocomposite filaments was done in terms of their structural properties through SEM, FTIR, XRD and DSC techniques. Nanocomposite filaments were also evaluated for changes in their mechanical properties and compared with the filament prepared without addition of SiO₂ nano particles.

The present research deals with production of Polypropylene/SiO₂ nanocomposite filament yarn by melt spinning concept using pilot plant. The present research has been limited to the yarn stage only. Melt spinning deals with the addition of nanoparticles precisely on the weight basis and mixed in twin screw extruder. Then extrusion through melt spinning pilot machine. This can lead towards the production of nanocomposite yarn. Changes in structural and mechanical properties were evaluated using standard test methods.

First, pure polypropylene filament was spun; the melt flow index (MFI) of the procured polypropylene chips was measured on melt flow indexer. The measured MFI is near to the MFI claimed by the manufacturer of the polypropylene chips. The average measured value of MFI is 15.58 and the MFI value as per material specification is 16.

Polypropylene nanocomposite filament yarns were prepared with various concentrations of SiO₂ nanoparticles viz. 0.1%, 0.3%, 0.5%, 0.7%, 1.0%, 1.25% and 1.5%. The nomenclature used during discussion for the samples prepared is as follow.

Table 4.6 Nomenclature of polypropylene SiO₂ nanocomposite filaments

| Sr. No. | SAMPLE | COMPOSITIONS |
|---------|--------|---|
| 1 | PP | Polypropylene without doping of SiO ₂ |
| 2 | NPP1 | Polypropylene with 0.1% doping of SiO ₂ |
| 3 | NPP2 | Polypropylene with 0.3% doping of SiO ₂ |
| 4 | NPP3 | Polypropylene with 0.5% doping of SiO ₂ |
| 5 | NPP4 | Polypropylene with 0.7% doping of SiO ₂ |
| 6 | NPP5 | Polypropylene with 1.0% doping of SiO ₂ |
| 7 | NPP6 | Polypropylene with 1.25% doping of SiO ₂ |
| 8 | NPP7 | Polypropylene with 1.5% doping of SiO ₂ |

PP: polypropylene, NPP: Nano silica loaded polypropylene

The prepared nanocomposite samples were compared with the sample prepared without SiO₂ nanoparticles, which is considered as control sample for further investigation. Prior pilot trials were undertaken to optimize the parameters involved during melt spinning for continuous spinning of filaments. Finally the control and the nanocomposite samples were prepared by using the optimized spinning parameters as given in table 3.6.

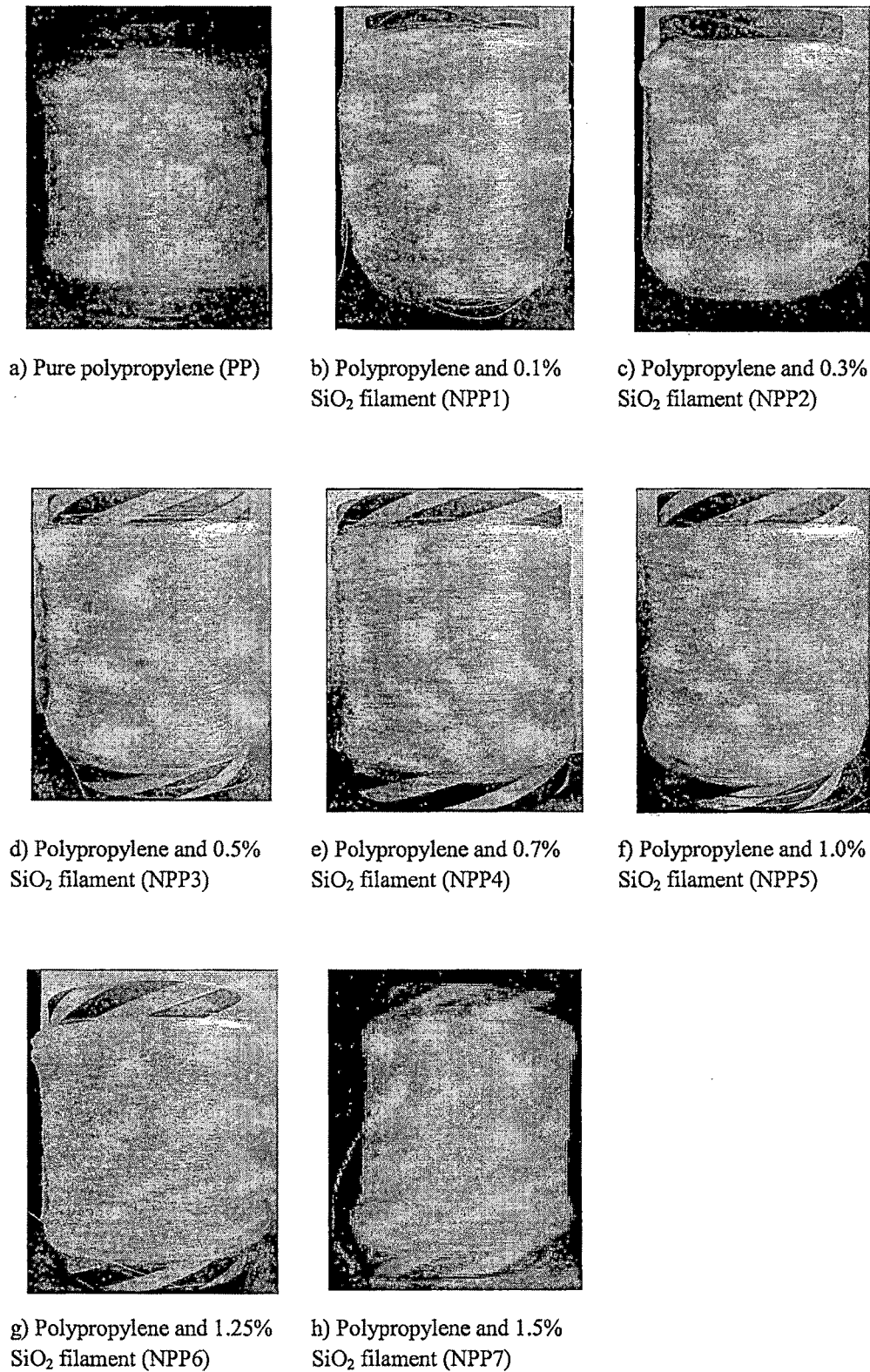


Figure 4.14 Polypropylene pure (a) and nanocomposite (b to h) filaments

4.2.1 STRUCTURAL ANALYSIS

4.2.1.1 Surface morphological analysis through SEM

The dispersion of SiO_2 nano particles on the surface of polypropylene filaments and inside the polymer matrix was observed by SEM micrographs. Figure 4.15 shows the SEM photograph of control sample, clear surface of filament can be seen at different magnifications. Figures 4.16 to 4.22 show the polypropylene filaments containing 0.1 to 1.5% SiO_2 nanoparticles by weight and figure 4.23 shows the cross sectional view of 0.7% concentration of SiO_2 nanoparticles prepared at melt spinning pilot plant.

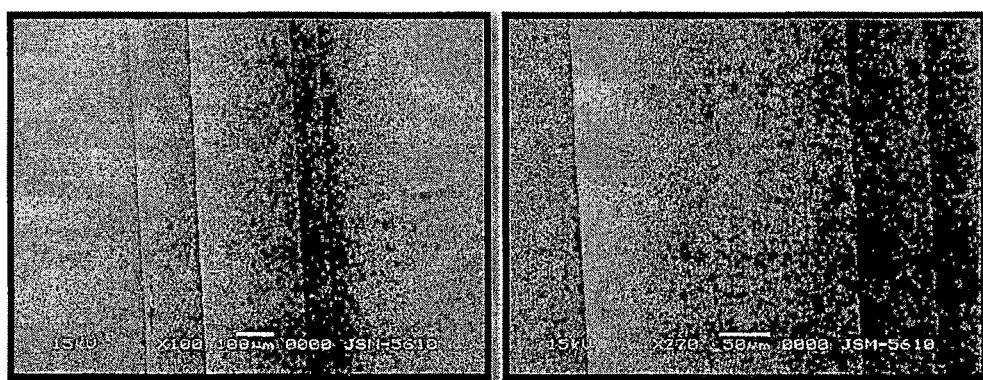


Figure 4.15 SEM photographs of Pure Polypropylene filaments (PP)

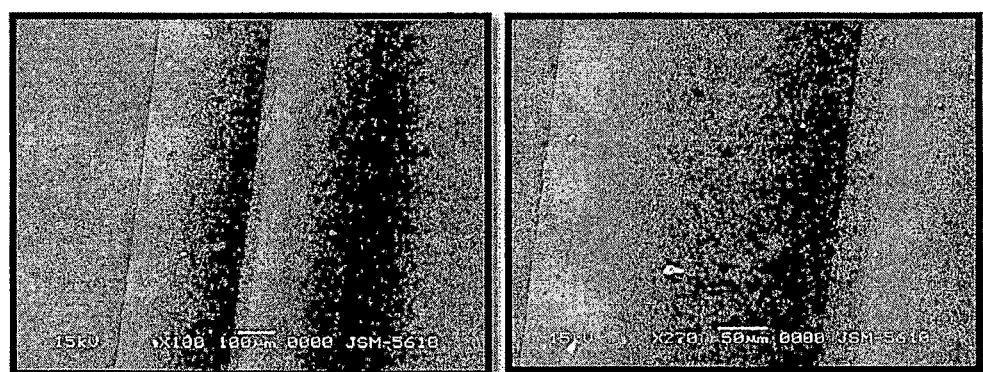


Figure 4.16 SEM photographs of PP filaments with 0.1% SiO_2 (NPP1)

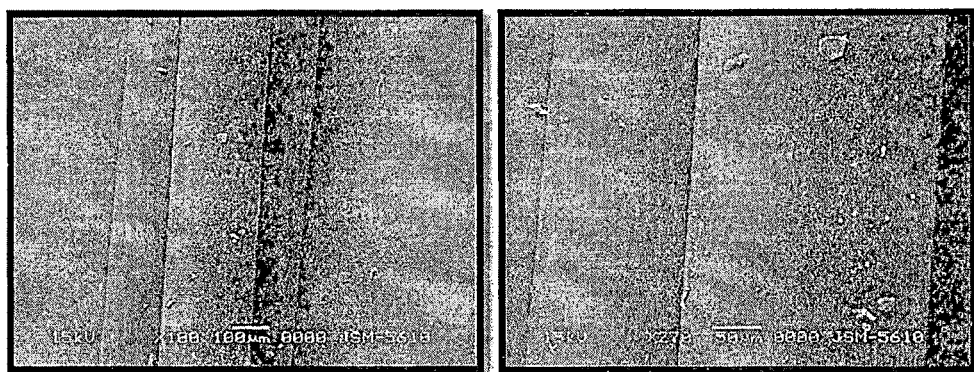


Figure 4.17 SEM photographs of PP filaments with 0.3% SiO₂ (NPP2)

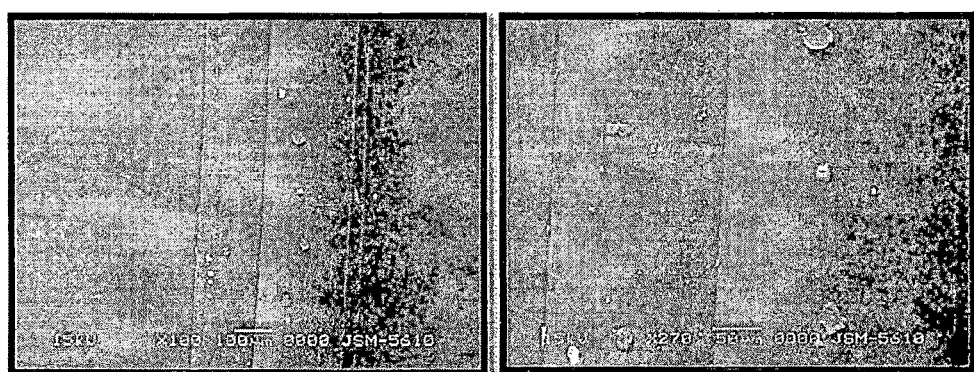


Figure 4.18 SEM photographs of PP filaments with 0.5% SiO₂ (NPP3)

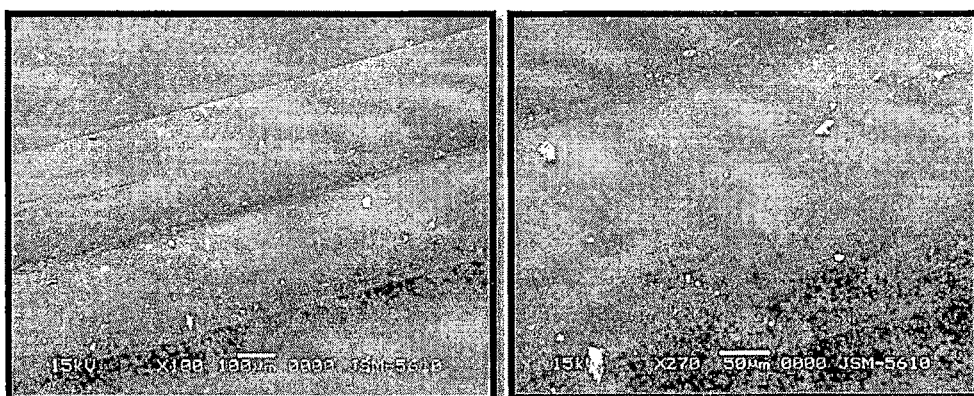


Figure 4.19 SEM photographs of PP filaments with 0.7% SiO₂ (NPP4)

The SEM micrographs confirm uniform distribution of nanoparticles. Some agglomeration of nano particles can be seen from 1% concentration. This agglomeration may be attributed to the increased concentration of SiO₂ nanoparticles and density difference of polypropylene and SiO₂. Polypropylene has density of 0.9

gm/cc and SiO_2 has density of 2.65 gm/cc [149]. The amount of agglomeration also increases with the increase in percentage concentration of SiO_2 nanoparticles.



Figure 4.20 SEM photographs of PP filaments with 1.0% SiO_2 (NPP5)

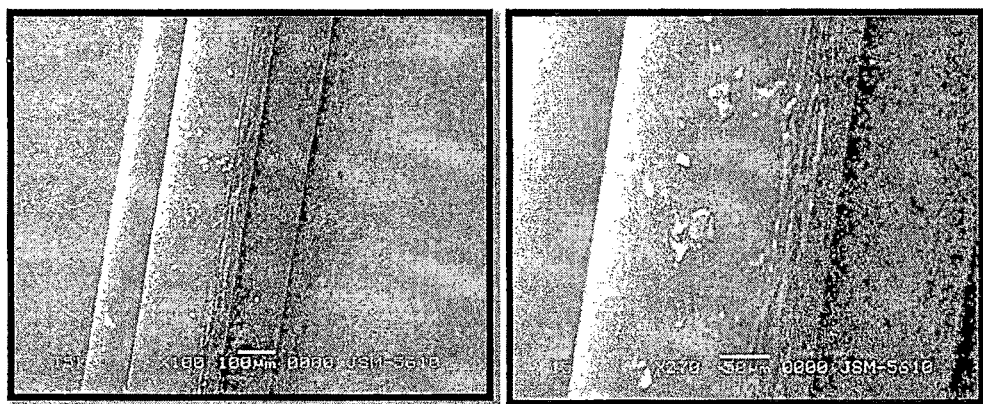


Figure 4.21 SEM photographs of PP filaments with 1.25% SiO_2 (NPP6)

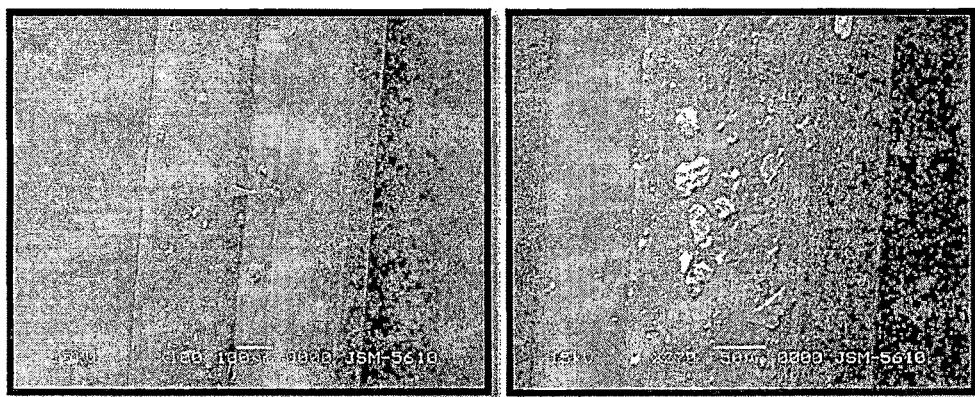


Figure 4.22 SEM photographs of PP filaments with 1.5% SiO_2 (NPP7)

The figure 4.23 shows the cross-sectional view of polypropylene silica nanocomposite filaments of 0.7% concentration of silica nano particles. In this view it can be seen that the distribution of the nanoparticles is throughout the structure of filament and also the distribution of nano particles is uniform.

The distribution of the nanoparticles within the structure has shown good uniformity for all the samples under consideration. Even number of nanoparticles induced within the structure has increased in direct proportion to SiO₂ content. The photographs show that even with the increase in percentage of SiO₂ content, good particle distribution was obtained.

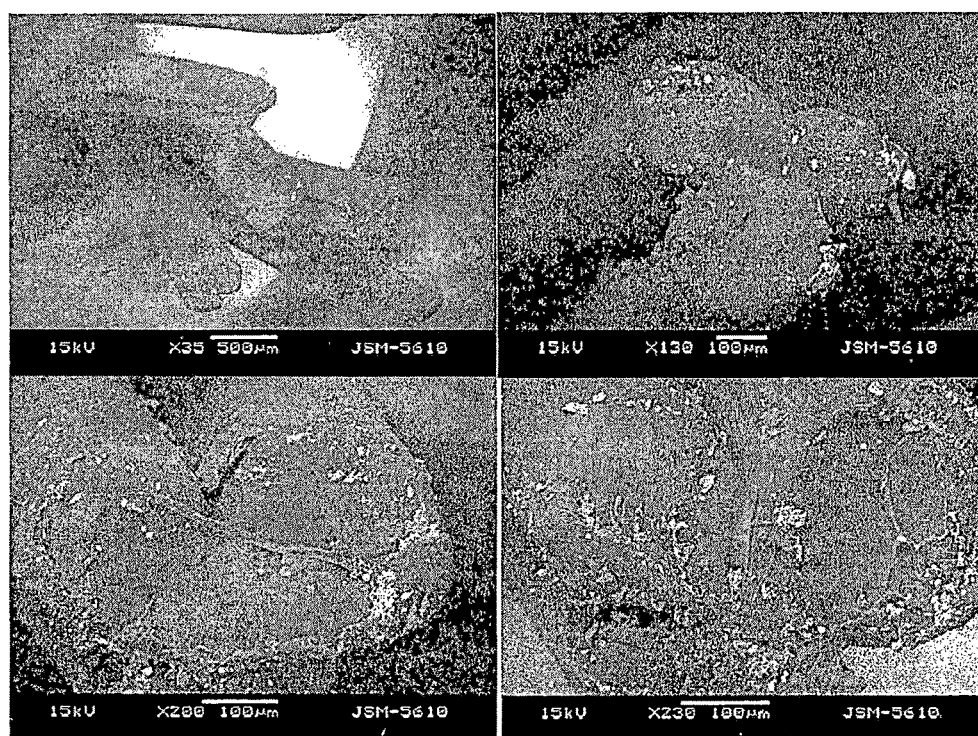


Figure 4.23 SEM cross-sectional photographs of PP filaments with 0.7% SiO₂ (NPP4)

4.2.1.2 Elemental analysis

The elemental analysis of pure polypropylene filament and polypropylene silica nanocomposite filament was performed on scanning electron microscope using Oxford-Inca software. The test results are shown in figure 4.24 and 4.25 and table 4.7 and 4.8. The presence of silica was confirmed by the elemental analysis curve, also the presence of oxygen in figure and table indicate that the silica is in the form of oxide or dioxide. Preparation of sample for testing as well as silicon dioxide nano particles may consist of impurities in final product like sodium, magnesium, chlorine, potassium, calcium and ferrous, as it has been reflected in elemental analysis. It may affect some properties of final product.

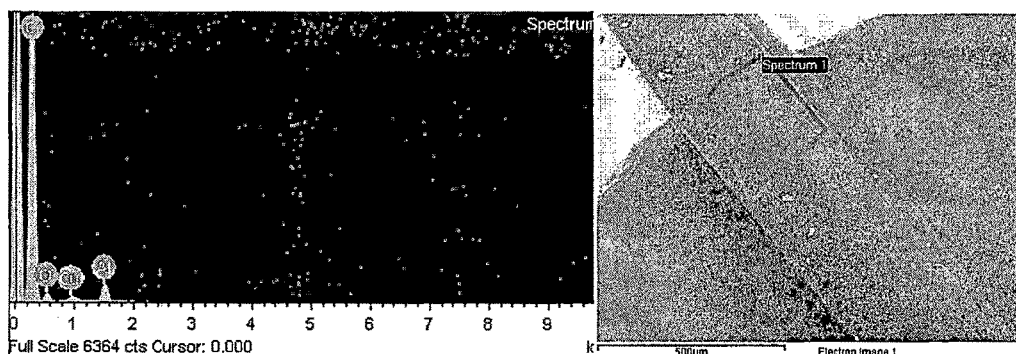


Figure 4.24 EDX spectrum of pure polypropylene filament

Table 4.7 Elemental analysis data of pure polypropylene filament

| Element | Weight% | Atomic% |
|--------------|---------------|---------|
| C K | 87.50 | 92.05 |
| O K | 8.30 | 6.56 |
| Al K | 2.08 | 0.97 |
| Cu L | 2.11 | 0.42 |
| Total | 100.00 | |

K: Confirm, L: Probable

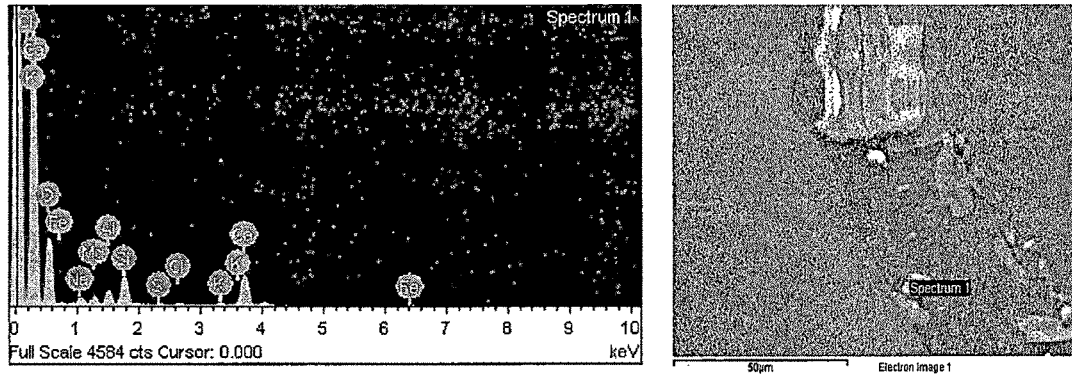


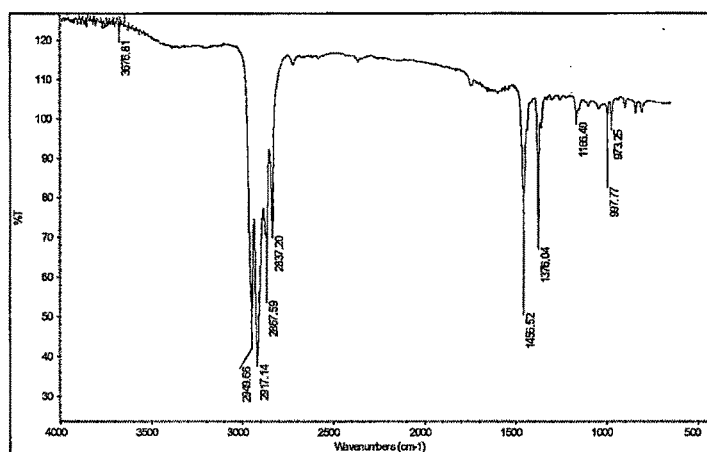
Figure 4.25 EDX spectrum of polypropylene silica nanocomposite filament

Table 4.8 Elemental analysis data of polypropylene silica nanocomposite filament

| Element | Weight% | Atomic% |
|--------------|---------------|---------|
| O K | 60.17 | 75.42 |
| Na K | 2.99 | 2.61 |
| Mg K | 2.50 | 2.06 |
| Al K | 3.90 | 2.90 |
| Si K | 8.86 | 6.33 |
| S K | 0.58 | 0.36 |
| Cl K | 0.87 | 0.49 |
| K K | 1.52 | 0.78 |
| Ca K | 16.66 | 8.34 |
| Fe K | 1.97 | 0.71 |
| Total | 100.00 | |

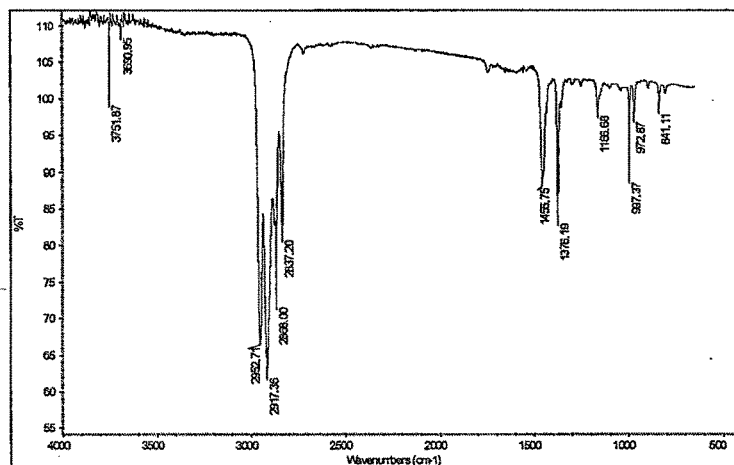
4.2.1.3 FTIR spectral analysis

The chemical compositions of the control sample and polypropylene/SiO₂ nanocomposite filaments were evaluated using FTIR Spectroscopy. Figure 4.26 (a) represents the IR absorption peak of pure polypropylene whereas figure 4.26 (b to i) represent IR absorption peaks of different concentrations SiO₂ nanoparticles in polypropylene nanocomposite filaments.

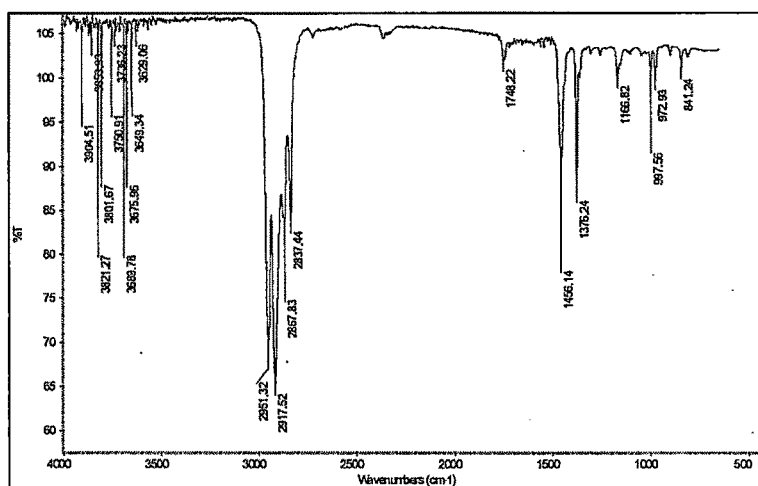


a) FTIR of Pure Polypropylene filaments (PP)

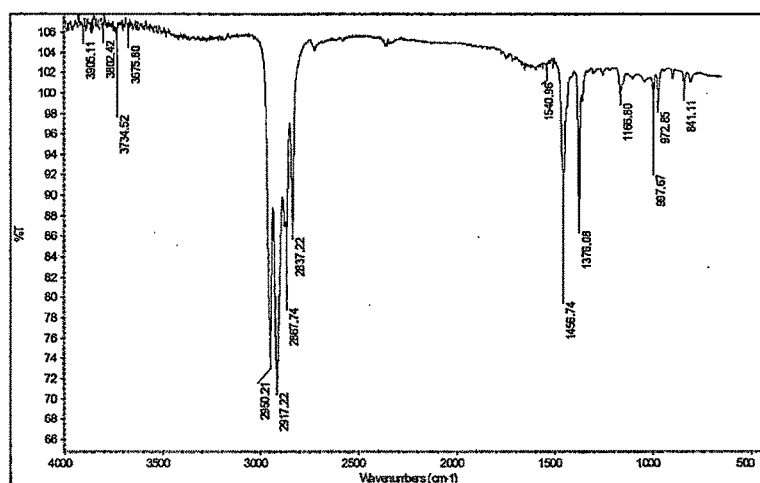
The chemical compositions of the pure polypropylene and polypropylene/silica nanocomposite filaments were evaluated using FTIR Spectroscopy. Figure 4.26(a) represents the IR characterization absorption peak of pure polypropylene filament, from which it can be seen that the major peaks associated were hydrogen bonded symmetric C-H stretching around 2949 cm⁻¹, asymmetric -CH stretching vibration at 2917 and 2867 cm⁻¹ [140], C-H stretching vibrations [141] at 2837 cm⁻¹, C=O stretching is observed at 1750 cm⁻¹, asymmetrical CH₂ bending [140] scissoring type at 1456 cm⁻¹, symmetrical CH bending [140] at 1376 cm⁻¹, the presence of polypropylene is confirmed at 973 cm⁻¹ which is irrespective of its tacticity, but at 997 and 1166 cm⁻¹ it is confirmed that the tacticity of polypropylene polymer is isotactic. Very few O-H stretch and free vibrations peak is observed around 3676 cm⁻¹.



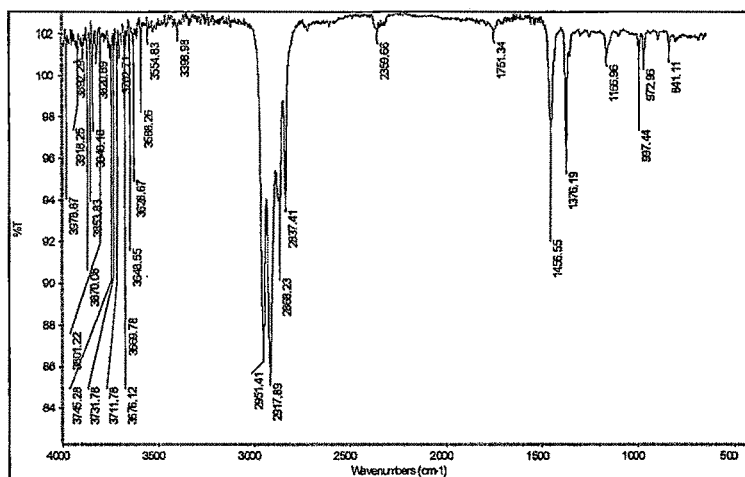
b) FTIR of PP filament with 0.10% SiO₂ (NPP1)



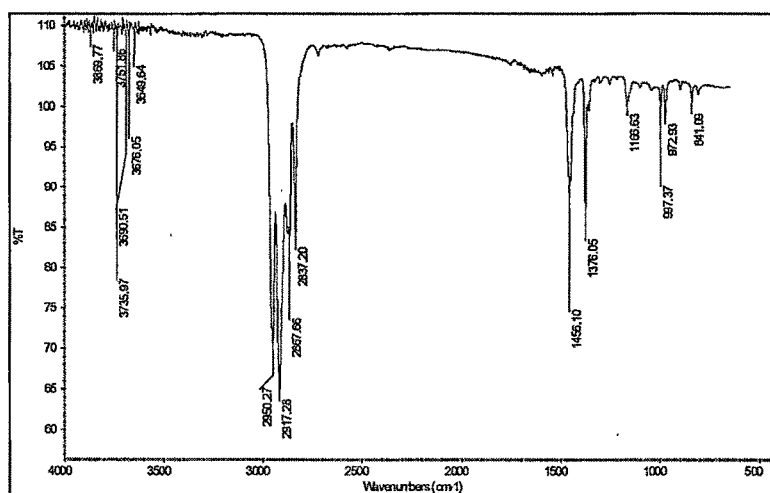
c) FTIR of PP filament with 0.30% SiO₂ (NPP2)



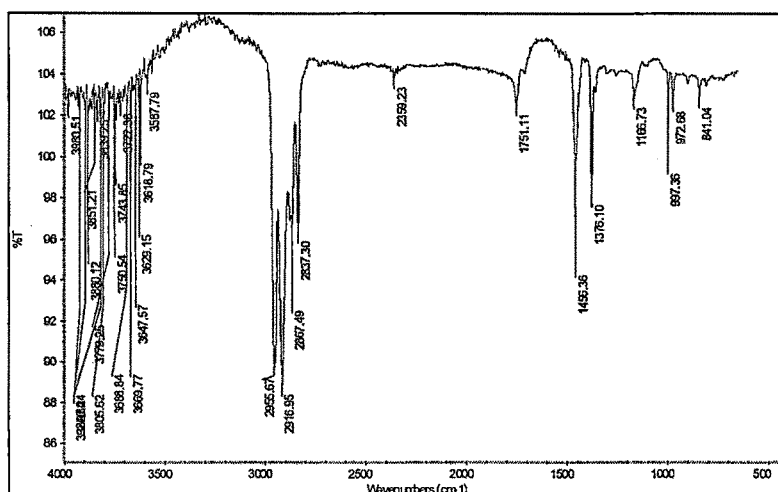
d) FTIR of PP filament with 0.50% SiO₂ (NPP3)



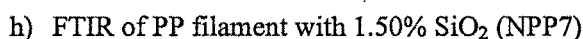
e) FTIR of PP filament with 0.70% SiO₂ (NPP4)



f) FTIR of PP filament with 1.00% SiO₂ (NPP5)



g) FTIR of PP filament with 1.25% SiO₂ (NPP6)



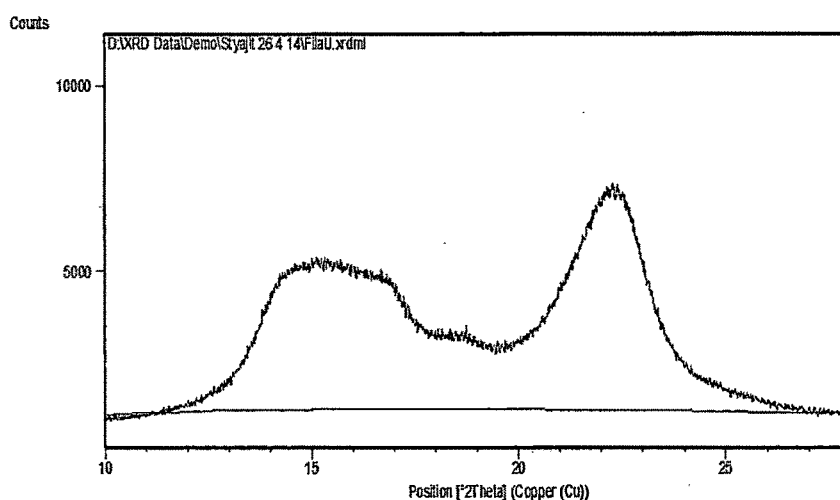
Investigation of structural and mechanical properties of Polymer-silica nanocomposite

Table 4.9 FTIR characterization peaks of pure polypropylene and polypropylene / Silica nanocomposite filaments.

| Groups | Wavenumber (cm ⁻¹) | | | | | | | |
|--|--------------------------------|---------|---------|---------|---------|---------|---------|---------|
| | PP | NPP1 | NPP2 | NPP3 | NPP4 | NPP5 | NPP6 | NPP7 |
| Si-O bending vibration | - | 841 | 841 | 841 | 841 | 841 | 841 | 841 |
| Presence of polypropylene irrespective of tacticity | 973 | 972 | 972 | 972 | 972 | 972 | 972 | 972 |
| Iso-tactic polypropylene | 997 | 997 | 997 | 997 | 997 | 997 | 997 | 997 |
| Iso-tactic polypropylene | 1166 | 1166 | 1166 | 1166 | 1166 | 1166 | 1166 | 1166 |
| Symmetrical CH bending | 1376 | 1376 | 1376 | 1376 | 1376 | 1376 | 1376 | 1376 |
| Asymmetrical CH ₂ bending-scissoring type | 1456 | 1456 | 1456 | 1456 | 1456 | 1456 | 1456 | 1456 |
| C=O stretching | 1750 | 1750 | 1748 | 1750 | 1751 | 1750 | 1751 | 1750 |
| CO ₂ formation | | | 2340 | | 2340 | | 2340 | 2340 |
| Intramolecular H-bridges | | | 2359 | 2359 | 2359 | 2359 | 2359 | 2358 |
| -CH stretching vibration | 2837 | 2837 | 2837 | 2837 | 2837 | 2837 | 2837 | 2837 |
| Asymmetric -CH stretching vibration | 2867 | 2868 | 2867 | 2867 | 2868 | 2867 | 2867 | 2868 |
| | 2917 | 2917 | 2917 | 2917 | 2917 | 2917 | 2916 | 2917 |
| Symmetric -CH stretching vibration | 2949 | 2952 | 2951 | 2950 | 2951 | 2950 | 2955 | 2956 |
| O-H stretch and free vibrations | 3500 | 3500 | 3500 | 3500 | 3500 | 3500 | 3500 | 3500 |
| | to 4000 | to 4000 | to 4000 | to 4000 | to 4000 | to 4000 | to 4000 | to 4000 |

4.2.1.4 X-ray diffraction analysis

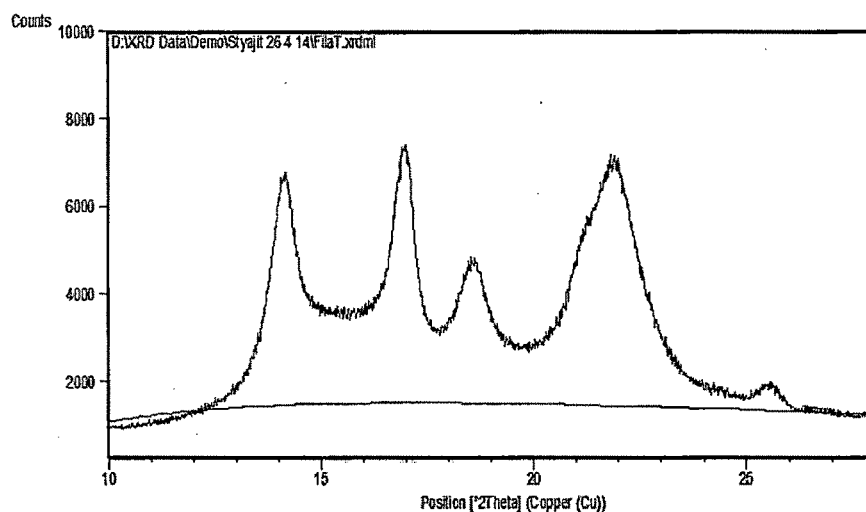
The X-ray diffraction patterns were taken on X'pert Pro PANalytical x-ray diffractometer. The XRD of both the fabrics was done within the 2θ range of 10° to 30° at the scan speed of 3° per minute at 25°C temperature, using $\text{Cu-K}\alpha$ radiation of wavelength 1.5406\AA . The diffraction profiles were obtained for individual samples. The XRD patterns are given in figure 4.27 and 4.28 for PP and NPP4 samples i.e. pure polypropylene filament and 0.7% nano silica in polypropylene filament respectively.



| Pos. [2θ] | Height [cts] | d-spacing [\AA] | Area[cts* 2θ] | Rel. Int. [%] |
|--------------------|--------------|----------------------------|-----------------------|---------------|
| 16.2515 | 2950.48 | 5.44974 | 2325.38 | 48.08 |
| 18.9598 | 1571.51 | 4.67694 | 3731.00 | 25.61 |
| 22.8988 | 6136.10 | 3.88056 | 4711.30 | 100 |

Figure 4.27 XRD pattern of pure polypropylene filament (PP)

In the XRD pattern of PP sample, only two broad prominent features are observed, which is an indication of a predominantly amorphous structure. The feature at 2θ value of 22.8988° has the highest intensity followed by very broad feature with elevation at 16.2515° and 18.9598° .



| Pos. [°2θ] | Height [cts] | d-spacing [Å] | Area [cts*°2θ] | Rel. Int. [%] |
|------------|--------------|---------------|----------------|---------------|
| 14.176 | 4547 | 6.24270 | 5940.13 | 82.31 |
| 16.872 | 5524 | 5.25059 | 7770.83 | 100 |
| 18.339 | 2503 | 4.83392 | 2561.03 | 45.32 |
| 22.454 | 2778 | 3.95646 | 3164.23 | 50.29 |
| 25.479 | 675 | 3.49319 | 410.37 | 12.22 |

Figure 4.28 XRD pattern of polypropylene silica nanocomposite filament (NPP4)

Figure 4.28 shows the XRD pattern of NPP4 sample, which clearly shows the change in XRD pattern due to addition of silica nano particles. It shows some sharper features with high intensity. Five prominent and wide peaks are observed. The peak at 2θ value of 16.872° has the highest intensity followed by 14.176° , 22.454° , 18.339° and 25.479° in that order.

Addition of silica nano particles result into enhanced crystallinity, which can be seen from the appearance of multiple peaks in the treated samples. The presence of silica nano particles might be affecting the kinetics of the interaction between the polymer and silica nanoparticles to give better crystallinity. Similar results have been observed by Srisawat, et al. that due to addition of nano silica, the polypropylene crystallinity increases on account of nucleating effect [153].

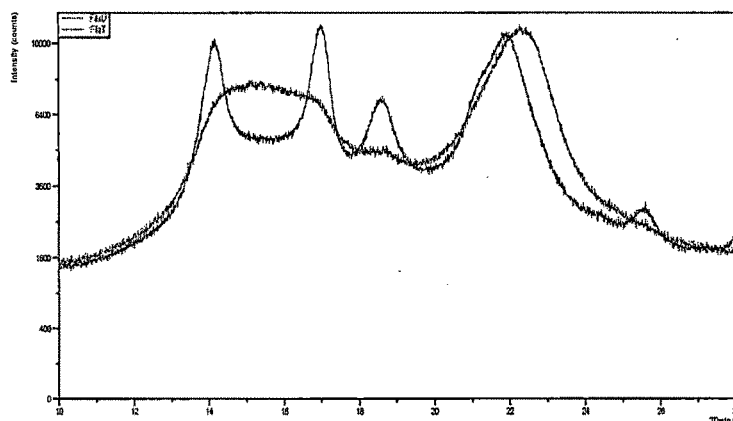


Figure 4.29 Combined XRD patterns of PP and NPP4 samples

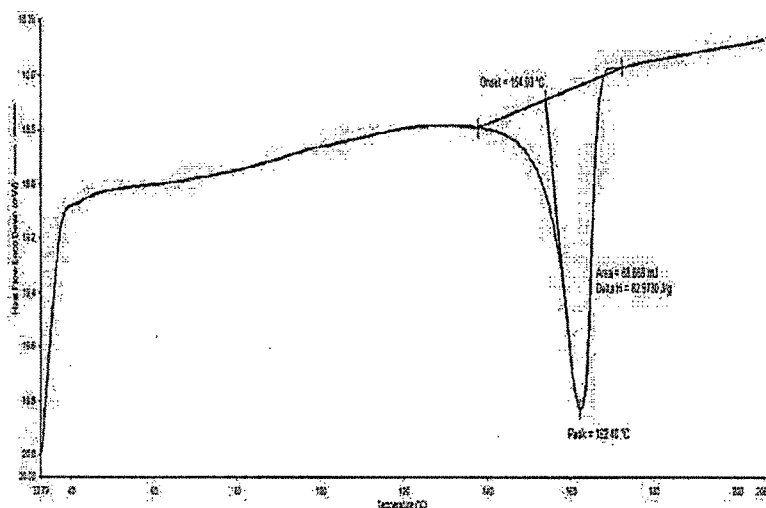
The 'd' values for the observed diffraction peak of silica is in close agreement with those reported for corresponding standard samples as reported in JCPDS data file no. 84-0384. The peak corresponding to the d-value of 3.9518 Å is an exact match with the obtained data.

4.2.1.5 Thermal analysis

Table 4.10 Effect of SiO₂ concentration on melting point of PP and enthalpy of melting (ΔH)

| Samples | SiO ₂ Concentration (%) | Melting Point T_m (°C) | Enthalpy ΔH (J/g) | Crystallinity $= \left(\frac{\Delta H}{(1-w_f)\Delta H^*} \right) \times 100$ (%) |
|---------|--|--------------------------------|------------------------------|---|
| CS | 0.00 | 162.40 | 82.97 | 39.70 |
| NPP1 | 0.10 | 161.99 | 85.50 | 41.03 |
| NPP2 | 0.30 | 162.94 | 87.96 | 42.62 |
| NPP3 | 0.50 | 162.97 | 87.92 | 42.36 |
| NPP4 | 0.70 | 161.63 | 90.52 | 43.75 |
| NPP5 | 1.00 | 163.13 | 94.23 | 45.31 |
| NPP6 | 1.25 | 162.45 | 82.92 | 40.28 |
| NPP7 | 1.50 | 161.42 | 81.41 | 38.97 |

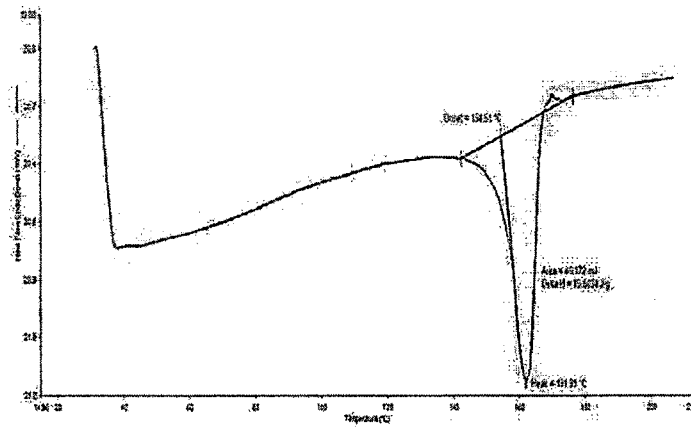
The thermal analysis was done on DSC 6000, by Perkin Elmer for all the samples. In the present study the concentration of nano silica selected was from 0.1% to 1.5%. The results of the analysis are reported in table 4.10 and the DSC curves are given in figure 4.26 (a to h).



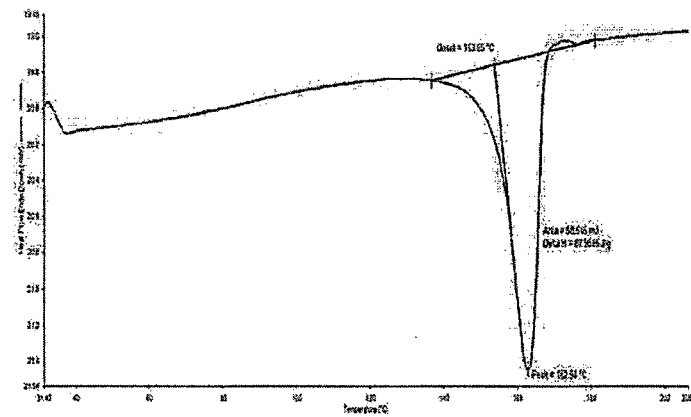
a) DSC curve of pure polypropylene filament (PP)

Figure 4.30 (a) shows the differential scanning calorimetry (DSC) curve of pure polypropylene filament. Here the pure polypropylene filament sample was heated at 10°C/min rate upto 300°C, in which it shows the melting temperature of the polypropylene filament as 162.4°C and the total heat required to melt i.e. enthalpy (ΔH) is 82.97 J/g, the % crystallinity calculated on the bases of enthalpy is 39.70%.

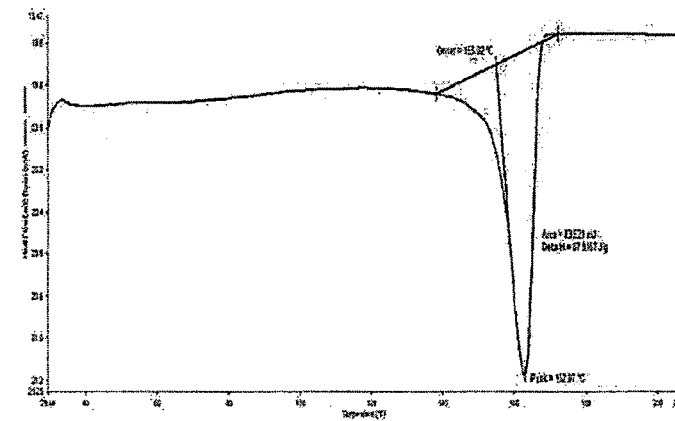
Figure 4.30 (b to h) shows the DSC curves of nanocomposite filaments of polypropylene and SiO₂ nano particles at different concentration levels like 0.1%, 0.3%, 0.5%, 0.7%, 1.0%, 1.25% and 1.5%. The melting temperature, enthalpy and % crystallinity of all filaments are given in table 4.10. The melting temperature of pure polypropylene filament is 162.4°C and there is no significant effect on melting temperature of all the nanocomposite filaments due to addition of silica nano particles. In case of polyamide film there was reduction in melting temperature at 1% silica concentration from 215°C to 209°C, which is explained in part-I. Even though there is agglomeration seen in 1%, 1.25% and 1.5% concentration sample of polypropylene nanocomposite filaments, there is no effect of this agglomeration on melting temperature like polyamide film.



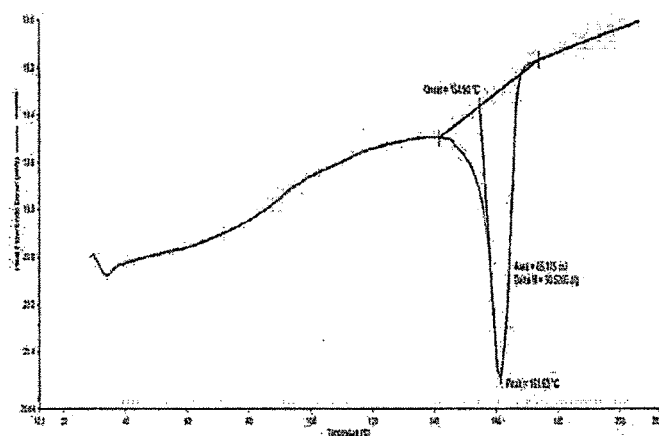
b) DSC curve of Polypropylene filament with 0.10% SiO₂ nanoparticles (NC - 2)



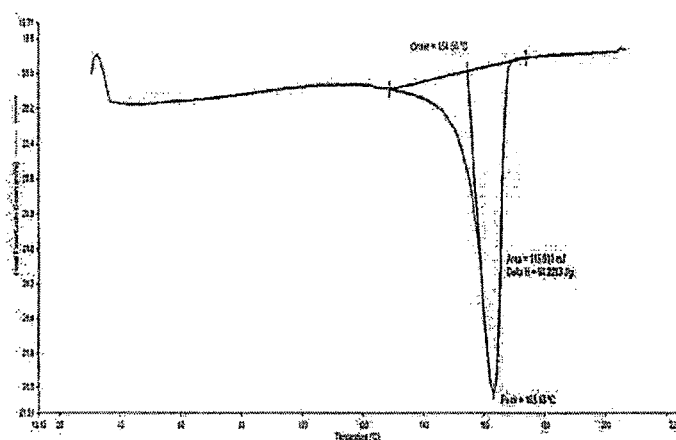
c) DSC curve of Polypropylene filament with 0.30% SiO₂ nanoparticles (NPP2)



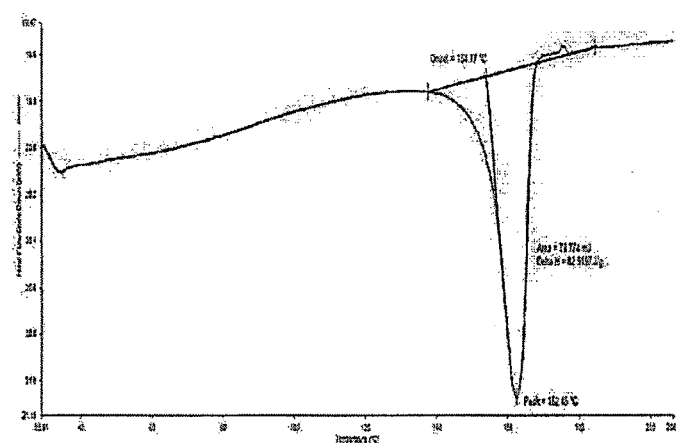
d) DSC curve of Polypropylene filament with 0.50% SiO₂ nanoparticles (NPP3)



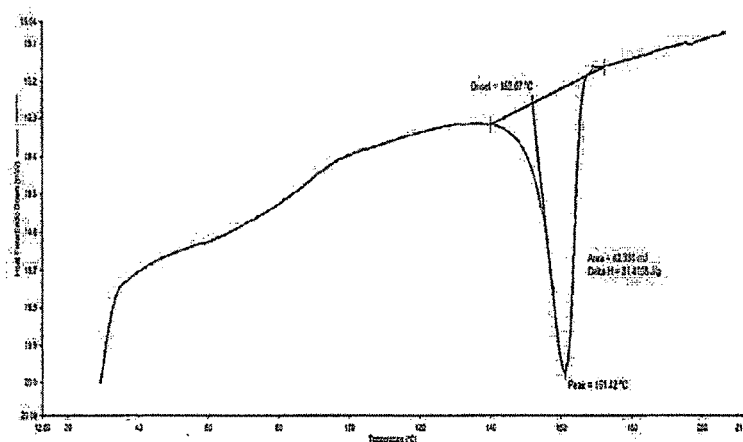
e) DSC curve of Polypropylene filament with 0.70% SiO₂ nanoparticles (NPP4)



f) DSC curve of Polypropylene filament with 1.00% SiO₂ nanoparticles (NPP5)



g) DSC curve of Polypropylene filament with 1.25% SiO₂ nanoparticles (NPP6)



h) DSC curve of Polypropylene filament with 1.50% SiO₂ nanoparticles (NPP7)

Figure 4.30 DSC curves of pure polypropylene (a) and polypropylene silica nanocomposite filaments (b to h)

It can be seen from the table 4.10 that with increase in SiO₂ nanoparticles concentration the ΔH value (enthalpy) has increased. The increase is in direct proportion to the SiO₂ nanoparticle concentration in polypropylene matrix i.e. upto 1% concentration and thereafter decreases. The same has led towards the increase in crystallinity value of the nanocomposite filament yarns in the same proportion [154]. Altan et al. [137] had reported that the increase in crystallinity with the increased SiO₂ nanoparticles concentration in polypropylene matrix was mainly attributed to the nucleation role of nanoparticles used. The results obtained in the present research have also followed the same trend.

The percentage change in enthalpy is found increasing by 3.05%, 6.01%, 5.97%, 9.10% and 13.57% with 0.1%, 0.3%, 0.5%, 0.7% and 1.0% concentration of nano silica in polypropylene filament respectively as compare to pure polypropylene filament. This may be due to increase in concentration and uniform distribution of nano particles in polymer matrix, which can be seen from the SEM micrographs. At 1.25% and 1.5% concentration of silica nano particles, the crystallinity is found reducing by 0.06% and 1.88% respectively as compare to pure polypropylene filament. This may be due to agglomeration of nano silica in polymer matrix and thus may not be allowing the formation of crystals, which has also seen in tenacity property, where with increase in concentration i.e. from 1%, the

tenacity is found reducing. This agglomeration of silica nano particles can also be seen from the SEM micrographs.

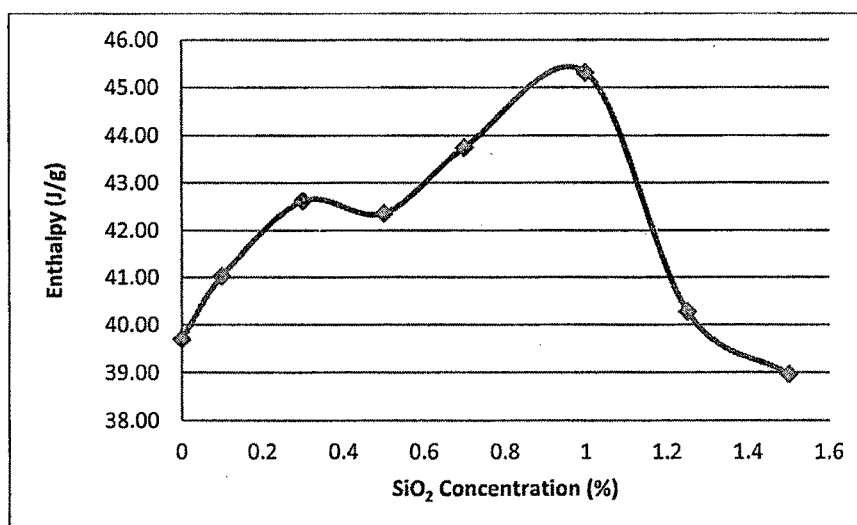


Figure 4.31 Effect of SiO₂ concentration on enthalpy of PP filament

The percentage change in crystallinity is found increasing by 3.35%, 7.36%, 6.70%, 10.20% and 14.13% with 0.1%, 0.3%, 0.5%, 0.7% and 1.0% concentration of nano silica in polypropylene filament respectively as compare to pure polypropylene filament. This may be due to increase in concentration and uniform distribution of nano particles in polymer matrix, which can be seen from the SEM micrographs. The XRD pattern also showing the increased number of peaks and their intensity also, this is an indication of increase in crystallinity. At 1.25% concentration of silica nanoparticles, the rise in crystallinity percentage is only 1.46% as compare to pure polypropylene filament, which is much less rise compare to lesser concentrations of nano particles polypropylene filaments. But at 1.5% concentration of silica nano particles the crystallinity is found reducing by 1.84% as compare to pure polypropylene filament. This may be due to agglomeration of nano silica in polymer matrix and thus may not be allowing bindings of polymer. This agglomeration of silica nano particles can also be seen from the SEM micrographs.

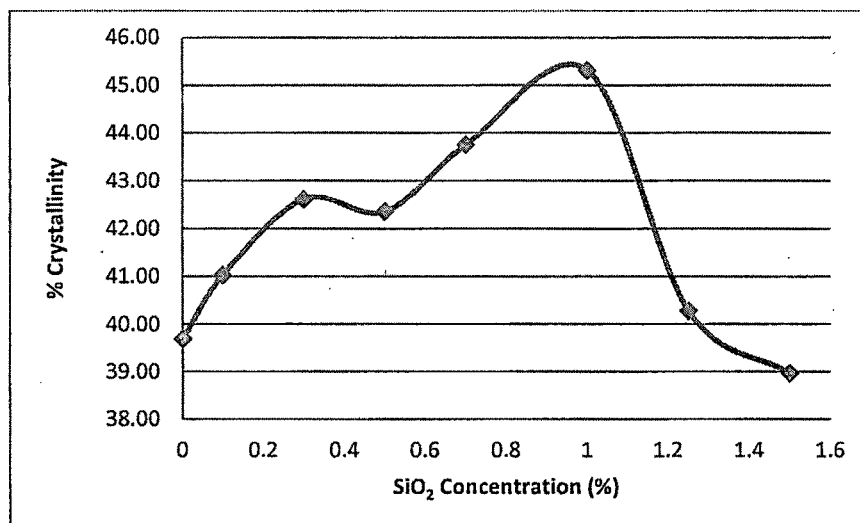


Figure 4.32 Effect of SiO₂ concentration on % crystallinity of PP filament

4.2.2 MECHANICAL PROPERTIES

The effect on mechanical properties i.e. tensile, young's modulus and work of rupture due to incorporation of silica nanoparticles in polypropylene filaments is studied here.

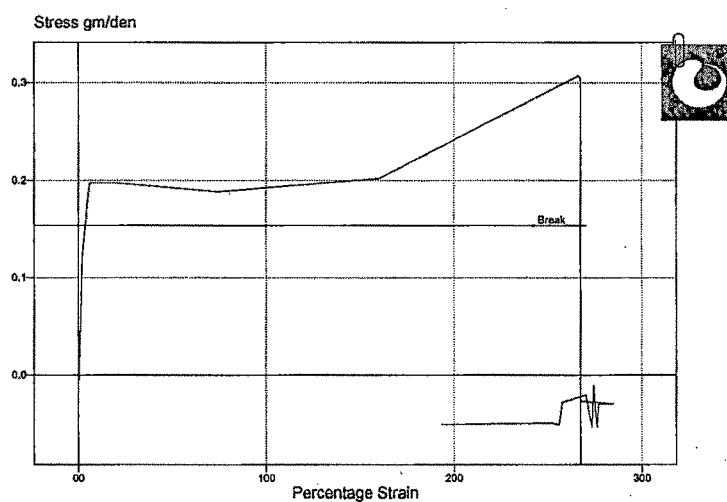
The silica nanoparticles were added in different proportions as 0.1, 0.3, 0.5, 0.7, 1.0, 1.25 and 1.5 percentages on weight bases.

4.2.2.1 Tensile strength

The tensile test was performed on Llyod LRX tensile testing machine and the stress strain curves of various sample tested are summarized in table 4.11 and shown in figure 4.33 below.

Table 4.11 Effect of SiO₂ nano particles on tensile property of polypropylene filaments

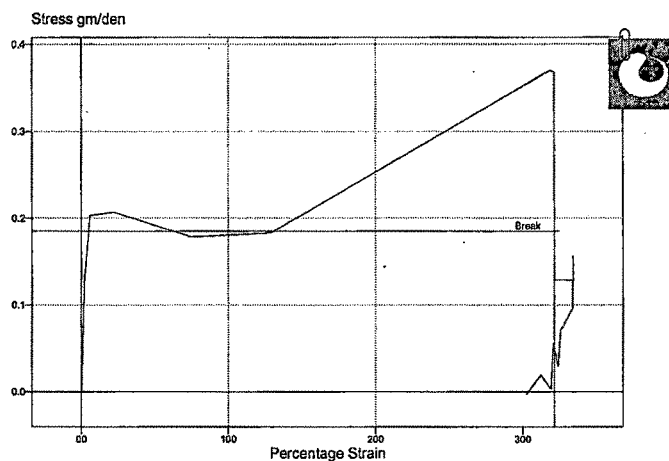
| SAMPLES | SiO ₂ Concentration (%) | Average Linear Density (Denier) | Maximum Load in gm | Tenacity in gm/den | % Elongation |
|---------|--|--|-----------------------|-----------------------|-----------------|
| CS | 0 | 2123.3 | 584.24 | 0.323 | 265.29 |
| NPP1 | 0.1 | 1572.53 | 641.94 | 0.375 | 380.2 |
| NPP2 | 0.3 | 616.79 | 288.63 | 0.464 | 585.51 |
| NPP3 | 0.5 | 999.75 | 388.4 | 0.488 | 218.39 |
| NPP4 | 0.7 | 677.84 | 364.66 | 0.542 | 286.93 |
| NPP5 | 1 | 1806.3 | 634.29 | 0.299 | 365.38 |
| NPP6 | 1.25 | 1717.6 | 438.66 | 0.279 | 311.82 |
| NPP7 | 1.5 | 1742.9 | 498.5 | 0.288 | 206.48 |



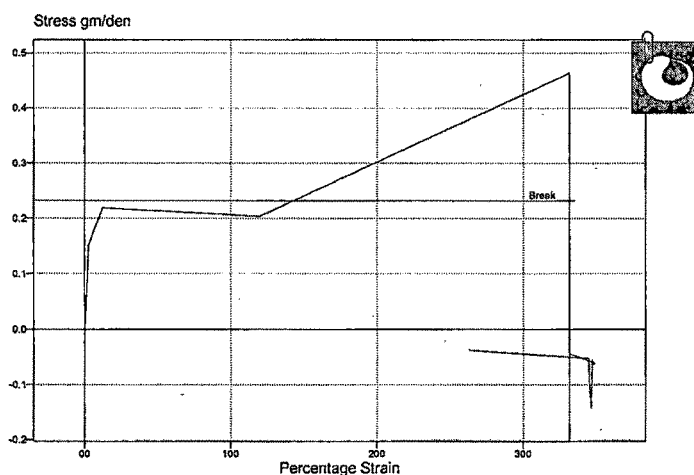
a) Pure Polypropylene filament (PP)

It is apparent from the results given in table 4.11 that as the concentration of silica nano particles increases, the strength of filament also increases. It may be due to the increased concentration of SiO₂ nanoparticles and stiff structure of silica particles, better dispersion and surface adhesion between the silicone dioxide and the polymer matrix causes

improvement in the tensile property of polypropylene filaments [137]. Nano particles in polymer structure impart stiffness to the polymer upto 0.7% concentration but beyond this concentration of SiO_2 the dispersion as well as surface adhesion between the nano particles and polymer structure may be getting disturbed, which result in decrease in tensile strength from 1% concentration and above [137].

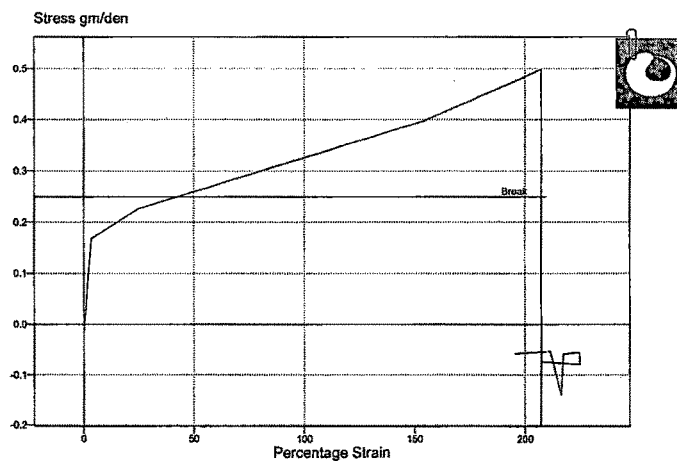


a) Polypropylene filament with 0.1% SiO_2 nanoparticles (NPP1)

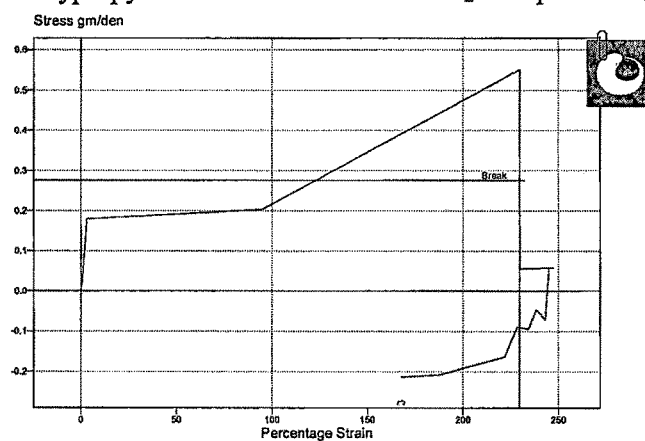


b) Polypropylene filament with 0.3% SiO_2 nanoparticles (NPP2)

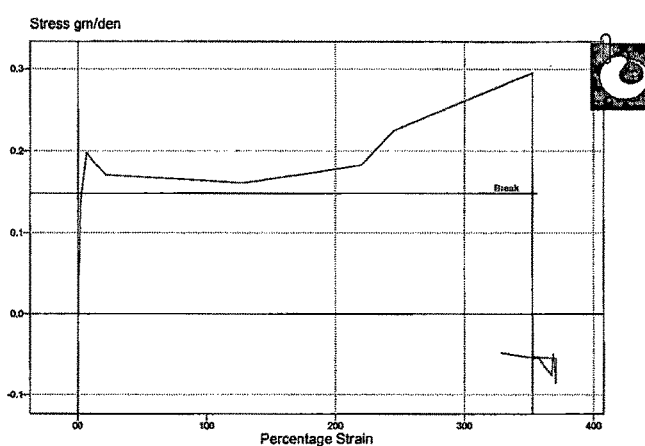
Results and discussion



c) Polypropylene filament with 0.5% SiO₂ nanoparticles (NPP3)



d) Polypropylene filament with 0.7% SiO₂ nanoparticles (NPP4)



e) Polypropylene filament with 1% SiO₂ nanoparticles (NPP5)

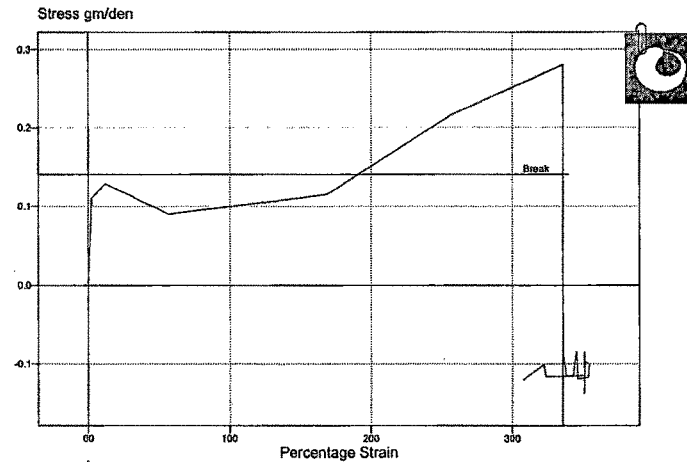
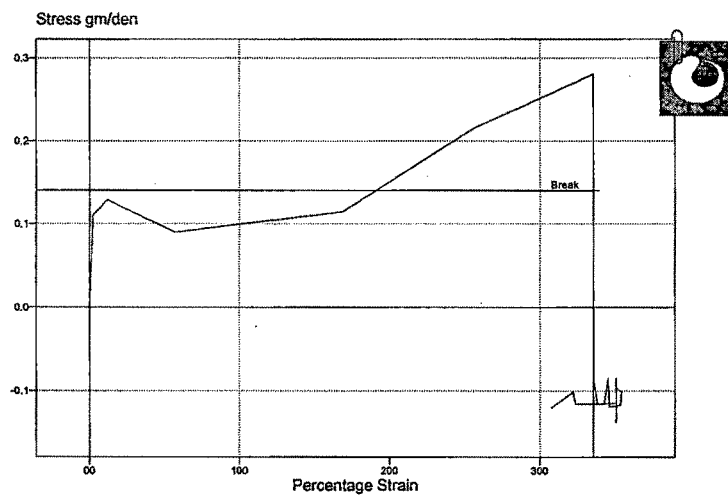
f) Polypropylene filament with 1.25% SiO₂ nanoparticles (NPP6)g) Polypropylene filament with 1.5% SiO₂ nanoparticles (NPP7)

Figure 4.33 Stress strain behavior of pure polypropylene (a) and polypropylene/SiO₂ nanocomposite filaments (b to h)

The percentage change in tenacity is found increasing by 16.10%, 43.65%, 51.08% and 67.8% with 0.1%, 0.3%, 0.5% and 0.7% concentration of nano silica in polypropylene filament respectively as compare to pure polypropylene filament as shown in figure 4.30. This may be due to increase in concentration and uniform distribution of nano particles in polymer matrix, which can be seen from the SEM micrographs [137]. It is also supported by the XRD pattern of NPP4 sample i.e. 0.7% nano silica concentration polypropylene filament, in which it has been observed that due to addition of nano silica the crystalline

peaks has increased. Above 0.7% concentration, it is observed that the tenacity decreases by 37.73%, 17.54% and 22.17% with 1%, 1.25% and 1.5% concentration of nano silica in polypropylene filament respectively as compare to pure polypropylene filament. This may be due to agglomeration of nano silica in polymer matrix and thus degrades the tenacity of nano composite polypropylene filaments, this agglomeration of silica nano particles can also be seen from the SEM micrographs [134].

Generally, tensile properties such as tensile strength, stress at break increases while elongation decreases [135, 136]. The increase in strength is seen upto 0.7% concentration of silica nano particles. This may be due to the uniform distribution and incorporation of silica nano particles in polypropylene polymer matrix. Above 0.7% concentration of silica nano particles, it has observed that the strength of filament decreases. This may be due to agglomeration of nano particles which may not be allowing to form compact structure [134].

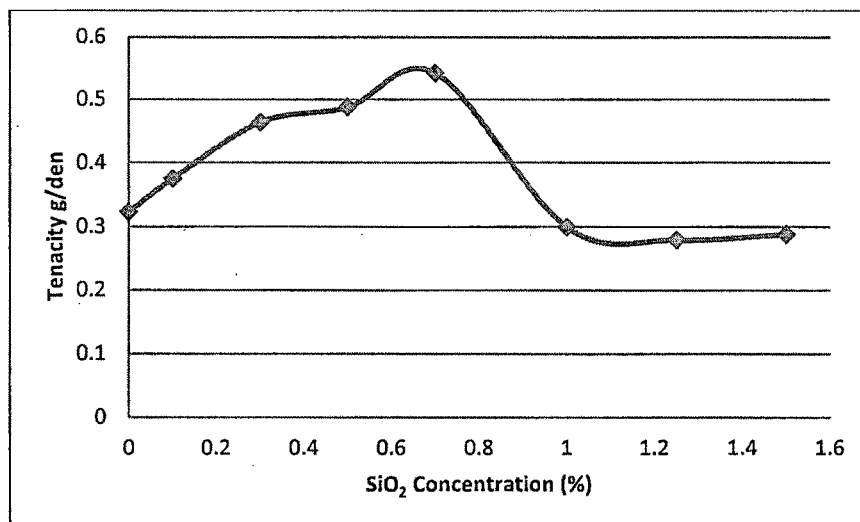


Figure 4.34 Tenacity of pure polypropylene and polypropylene silica nanocomposite filament

The load elongation curves of these undrawn pure polypropylene and silica nano composite polypropylene filaments are shown in figure 4.33 (a to h). The neck phenomenon is observed in all polypropylene filaments, which may be due to slow spinning speed i.e. 400 rpm, caused into amorphous structure. Overall each curve may be divided into three regions. In the first region, the load elongation relationship is approximately linear and the deformation is more or less reversible i.e. elastic nature. The load then reaches a maximum

and falls slightly. After this, filament deforms plastically under constant load conditions and the deformation is not recoverable. The material draws through a neck and the reduced cross-sectional area spreads through the neck through the whole length of the specimen. Finally, as the breaking point is approached, the stress rises sharply with a small increment in strain, signifying strain hardening before catastrophic failure occurs [155].

The increase in tensile strength of nano composites might be due to the phenomenon of reinforcement effect at nanoscopic level. All the samples under consideration are low oriented yarns. So, they need further drawing before application, which will alter its tensile behavior further.

4.2.2.2 Young's modulus and work of rupture

Table 4.12 Effect of nano silica on young's modulus and work of rupture

| Sample | % Concentration of nano SiO ₂ | Young's Modulus (g/den) | Work of rupture at maximum load (kgf.mm) |
|--------|---|-------------------------------|--|
| PP | 0.0 | 0.030 | 69.28 |
| NPP1 | 0.1 | 0.031 | 29.03 |
| NPP2 | 0.3 | 0.045 | 33.11 |
| NPP3 | 0.5 | 0.050 | 39.97 |
| NPP4 | 0.7 | 0.052 | 78.22 |
| NPP5 | 1.0 | 0.027 | 54.14 |
| NPP6 | 1.25 | 0.010 | 61.85 |
| NPP7 | 1.5 | 0.029 | 39.14 |

The table 4.12 and figure 4.35 show the young's modulus (Meredith's method) of pure polypropylene filament and nano silica loaded polypropylene filaments. The pure polypropylene filament is showing lower young's modulus i.e. 0.030 g/den than the silica loaded polypropylene nanocomposite filaments i.e. 0.031, 0.045, 0.050 and 0.052 g/den for 0.1%, 0.3%, 0.5% and 0.7% concentration of nano silica particles in polypropylene filament. Above 0.7% concentration i.e. 1%, 1.25% and 1.5%, the drop in young's modulus to 0.027, 0.010 and 0.029 g/den is observed.

The young's modulus is found increased with addition of silica nano particles and also there is increase in young's modulus with increase in percentage loading of silica nano particles i.e. upto 0.7% concentration. It means that initially the load bearing capacity of nanocomposite filament increases with addition of silica nanoparticles. Above 0.7% concentration of silica nano particles, the drop in young's modulus is observed. This drop may be due to agglomeration of silica nano particles, which may not be allowing to form compact structure. Due to which the structure would become brittle and can break easily, which has also been supported by reduced tenacity of these filaments.

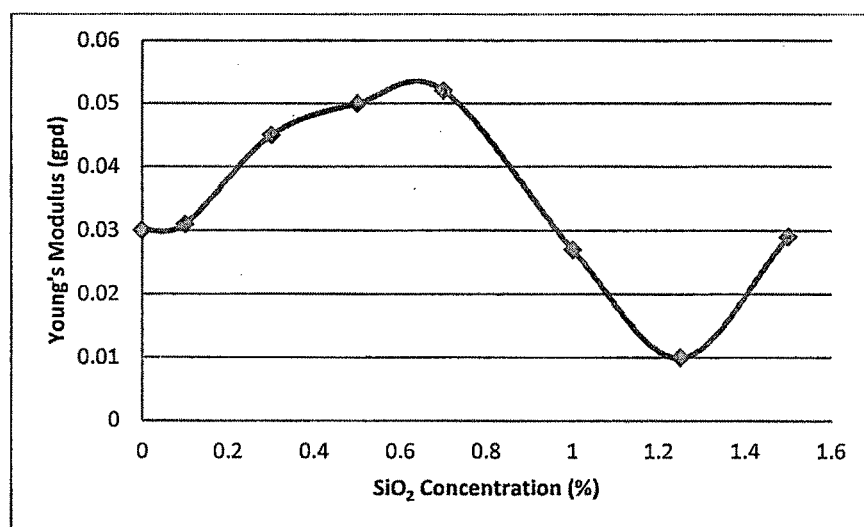


Figure 4.35 Effect of nano silica on young's modulus of treated and untreated polypropylene filaments

The work of rupture is energy or work required to break the specimen, it is a measure of the "toughness" of the material. The area under the load-elongation curve represents the work done in stretching the material to breaking point. The work of rupture value indicates the resistance of the material [148]. Table 4.12 and figure 4.36 show the work at maximum load, of pure polypropylene filament and nano silica loaded polypropylene filaments. The work required to break the pure polypropylene filament (PP) is 69.28 kgf.mm. Sample NPP1, NPP2 and NPP3 are showing reduced work of rupture at maximum load as compare to PP sample, which means that to

break these samples less energy is required. Sample NPP4 i.e. 0.7% concentration of nanosilica is showing increased work of rupture i.e. more energy is required to break this sample which means that this sample became more tough and also overall this sample is showing good property in all aspects i.e. tenacity and young's modulus. Above 0.7% concentration sample again there is reduction in work of rupture, it may be due to agglomeration of nano particles and making the filament brittle and break easily with less energy, it may be due to agglomeration of nano particles, agglomeration can be seen from the SEM micrograph in figure 4.20 to 4.22. Overall the work of rupture of the NPP4 sample of 0.7% nano silica loaded polypropylene filament is showing rise as compare to all other samples. Higher nano silica loaded polypropylene filament would not be allowing the material to become compact due to agglomeration of the nano particles and becoming more brittle, which would be hindering the development of compact structure. Similar trend has been observed in case of polyamide silica nanocomposite films, in which due to addition of silica nano particles the strength, young's modulus has found increasing upto 0.7% concentration and thereafter there is decrease in these properties observed.

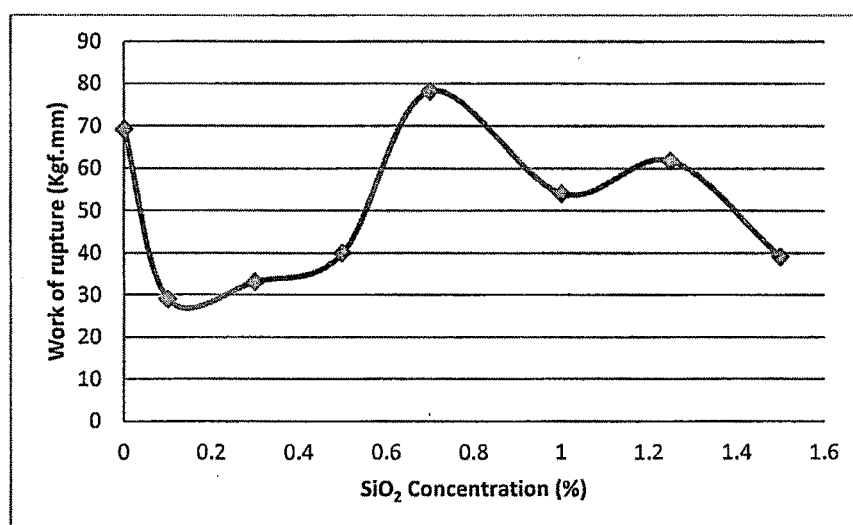


Figure 4.36 Effect of nano silica on work of rupture of treated and untreated polypropylene filaments

4.3 PART – III: POLYMER SILICA NANOCOMPOSITE FABRIC

Polymer Silica nanocomposite fabrics were prepared by incorporating different quantities of silica nano particles to polymeric fabric i.e. polyester fabric by pad-dry-cure method. The prepared nanocomposite fabrics were analyzed in terms of change in their structural and mechanical properties. Then the comparison was done with the pure polyester fabric.

In this part, the basic polymer was changed to polyester in fabric form, and the concentration of silica nano particles is kept as 1 gpl, 2.5 gpl and 5 gpl. The polyester fabric with different proportions of silica nanoparticles were prepared by pad-dry-cure method. The evaluation of prepared polymer silica nanocomposite fabric was done in terms of their structural properties through SEM, FTIR, XRD and DSC techniques. Nanocomposite fabrics were also evaluated for changes in their mechanical properties and compared with the pure polyester fabric. The nomenclature used during discussion for the samples prepared is as given in table 4.13.

Table 4.13 Compositions of polypropylene SiO₂ nanocomposite filament

| Sr. No. | SAMPLE | COMPOSITIONS |
|---------|--------|--|
| 1 | PT | Polyester fabric without SiO ₂ |
| 2. | NPT1 | Polyester fabric with 1 gpl SiO ₂ |
| 3 | NPT2 | Polyester fabric with 2.5 gpl SiO ₂ |
| 4 | NPT3 | Polyester fabric with 5 gpl SiO ₂ |

PT: polyester, NPT: Nano silica loaded polyester

4.3.1 STRUCTURAL ANALYSIS

4.3.1.1 Surface morphological analysis through SEM

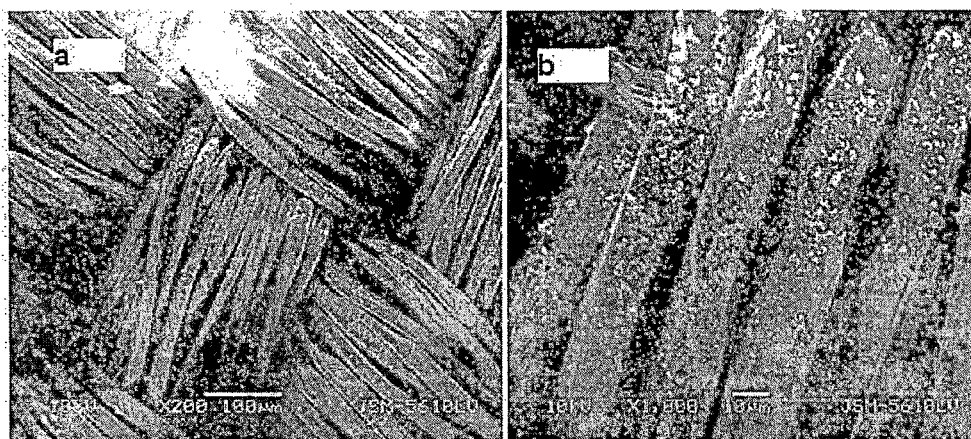


Figure 4.37 SEM microphotographs of polyester fabric treated with silica nano particles

The surface morphology of the treated polyester fabric sample was observed on scanning electron microscopy. The result is shown in figure 4.37, the nano scale silica particles can be clearly seen well distributed on the surface of polyester sample. The particle size plays a primary role in determining their adhesion to the fibre. It is reasonable to expect that the largest particle agglomerates will be easily removed from the fibre surface, while the smaller particle will penetrate deeper and adhere strongly into the fabric matrix. As reported by Wang et. al [41] in their study in 2004 that nano particles have large surface area to volume ratio, which makes it easy for them to attach to fibres or fabrics and increase the durability of the functions imparted by the particles.

4.3.1.2 FTIR spectral analysis

The chemical compositions of the treated and untreated polyester fabrics were evaluated using Fourier transform infrared spectroscopy (FTIR) Nicolet is10 FT-IR Spectrometer (Thermo Scientific). IR characterization absorption peaks of untreated and treated fabrics are shown in figure 4.38 and 4.39 respectively.

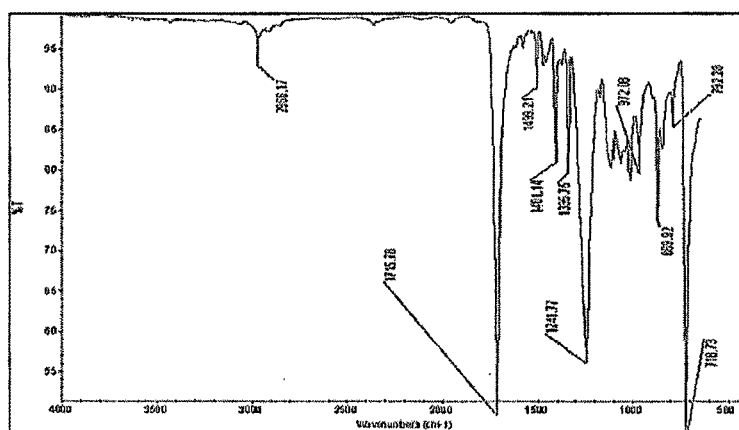


Figure 4.38 IR absorption peaks of untreated polyester fabric (PT)

Table 4.14 and figure 4.38 represents the IR characterization absorption peak of pure polyester fabric, from which it can be seen that the peaks associated were 2966 cm^{-1} shows C-H stretching, 1715 cm^{-1} shows C=O vibration, 1499 cm^{-1} shows skeletal ring stretching vibration of aromatic and hetero aromatic ring, 1401 cm^{-1} of aromatic ring, 1335 cm^{-1} & 1021 cm^{-1} shows carboxylic ester or anhydride, 1021 cm^{-1} indicates the presence of O=C-O-C or secondary alcohol, 1241 cm^{-1} shows C-O stretch alcohols carboxylic acid, 972 cm^{-1} is of C=C stretching, 869 cm^{-1} peak shows five substituted H in benzene, 792 cm^{-1} shows C-H stretching in aromatic ring and 718 cm^{-1} shows C-H rock alkane. The main structure of the polyester sample had ester, alcohol, anhydride, aromatic ring and heterocyclic aromatic rings. Alcohol was able to react with anhydride and produce ester groups. This is a reason that there is still alcohol and anhydride as residual reactants left in the polyester. The peak at 1409 cm^{-1} corresponded to the aromatic ring which is a stable group. It was the characteristic absorption peak of PET. The peak at 1715 cm^{-1} was assigned to the ester group.

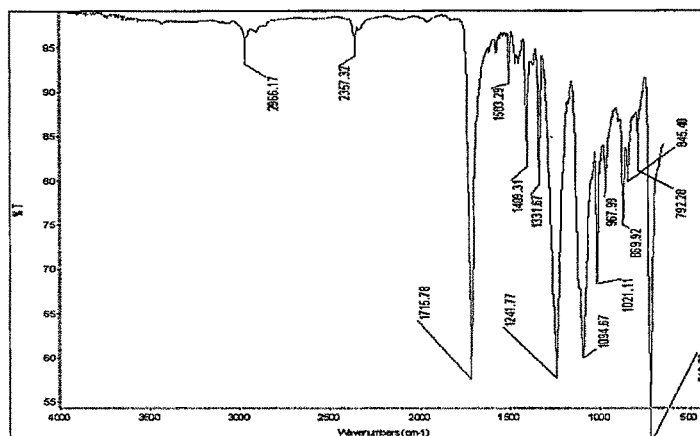


Figure 4.39 IR absorption peaks of treated polyester fabric (NPT3)

Peaks shown by pure polyester fabric are identical in polyester silica nanocomposite fabric as shown in figure 4.39, additionally the nanocomposite fabric shown the peaks of silica at 845 cm^{-1} corresponds to Si-O-Si [143] bending vibration, band at 1094 cm^{-1} correspond to asymmetric stretching vibration of Si-O-Si [144, 86] band, Si-C stretching belongs to 2357 cm^{-1} [140].

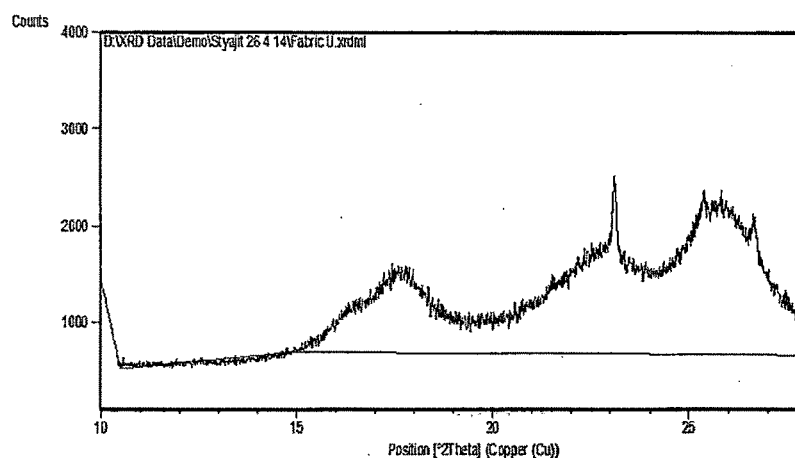
Table 4.14 FTIR characterization peaks of pure polyester and polyester/Silica nanocomposite fabric

| Groups | Wave number (cm^{-1}) | |
|---|----------------------------------|------|
| | PT | NPT3 |
| C-H rock alkane | 718 | 718 |
| C-H stretching in aromatic ring | 792 | 792 |
| Si-O-Si bonds vibration | | 845 |
| H in benzene | 869 | 869 |
| C=C stretching | 972 | 967 |
| Carboxylic ester or anhydride, O=C-O-C or secondary alcohol | 1021 | 1021 |

| | | |
|---|------|------|
| Si-O-Si asymmetric stretching vibration band | | 1094 |
| C-O stretch alcohols carboxylic acid | 1241 | 1241 |
| Carboxylic ester or anhydride | 1335 | 1331 |
| Aromatic ring (PET) | 1401 | 1409 |
| Skeletal ring stretching vibration of aromatic and hetero aromatic ring | 1499 | 1503 |
| C=O stretch (strong), unsaturated ester group (polyester) | 1715 | 1715 |
| Si-C stretching | | 2357 |
| C-H stretching | 2966 | 2966 |

4.3.1.3 X-ray diffraction analysis

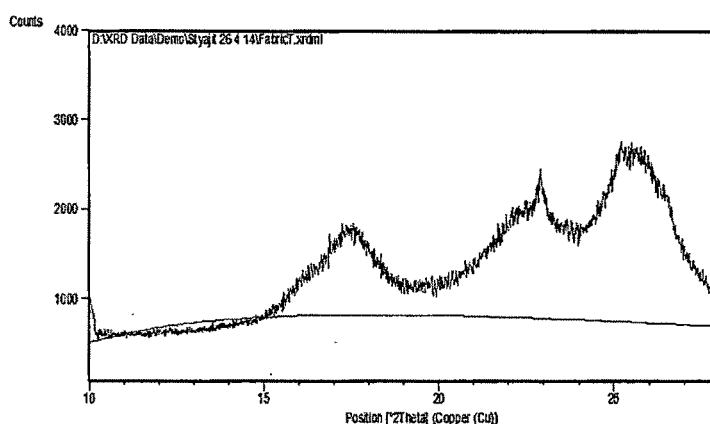
The characterization of treated and untreated polyester fabrics was done using PANalytical XRD. The XRD of both the fabrics was done within the 2θ range of 10° to 30° at the scan speed of 3°C per minute at 25°C temperature, using $\text{Cu-K}\alpha$ radiation of wavelength 1.5406 \AA . The diffraction profiles were obtained for individual samples. The X-Ray Diffractometer X'pert Pro PANalytical, Singapore make was used. The XRD patterns are given in figure 4.40 and 4.41 for PT and NPT3 samples i.e. pure polyester fabric and 5 gpl nano silica in polyester fabric, respectively.



| Pos. [°2 θ] | Height [cts] | d-spacing [Å] | Area [cts*°2 θ] | Rel. Int. [%] |
|---------------------|--------------|---------------|-------------------------|---------------|
| 17.66 | 854 | 5.09492 | 1650.99 | 62.13 |
| 23.11 | 719 | 3.87573 | 92.96 | 100 |
| 25.89 | 1179 | 3.45912 | 1203.79 | 87.52 |
| 26.6 | 981 | 3.41702 | 438.67 | 82.27 |

Figure 4.40 XRD pattern of pure polyester fabric (PT)

XRD pattern of PT sample as shown in figure 4.40 shows semi crystalline state of the material. Four prominent features are observed. One distinct crystalline peak is observed due to which the semi crystalline nature of polyester fibre may be considered. Some broadness in peak is also observed in rest of the peaks, but they by and large denote the amorphous nature of fibre. The peak at 2θ value of 23.11° has the highest intensity followed by 25.89° , 26.6° and 17.66° and these peaks are indicative of polyester polymer [156].



| Pos. [°2 θ] | Height [cts] | d-spacing [Å] | Area [cts*°2 θ] | Rel. Int. [%] |
|---------------------|--------------|---------------|-------------------------|---------------|
| 17.2642 | 813 | 5.11714 | 1116.17 | 66.67 |
| 22.9302 | 1108 | 3.91579 | 1407.17 | 83.27 |
| 25.7797 | 1525 | 3.50489 | 3012.15 | 100 |
| 26.0695 | 309 | 3.44348 | 62.95 | 81.48 |

Figure 4.41 XRD pattern of polyester silica nanocomposite fabric (NPT3)

The incorporation of silica nano particles lead to the development of some kind of force which drifts the atomic planes, such that the d-value increases. From the figure 4.42 it can be seen that the intensities in the treated sample is on the lower side compared to the untreated samples. There is a shift in the peak 2θ values towards the lower side in general, indicating a change in d-values across the range, to the same extent. Hence, the presence of silica nano particles affects the structure of material in terms of atomic plane spacing. The SEM micrographs show the incorporation of silica nano particles well dispersed on the surface of fabric. The d-values for the observed diffraction peak of silica is in close agreement with those reported for corresponding standard samples as reported in JCPDS data file 84-0384. Here the peak corresponding to the d-value of 3.4224 \AA is in agreement.

Sosa et. al [129] reported that as each crystalline material including the semi crystalline polymers as well as metal and metal oxide particles and layered silicate nano particles have a characteristic atomic structure, it will diffract X-ray in a unique characteristic diffraction order or pattern.

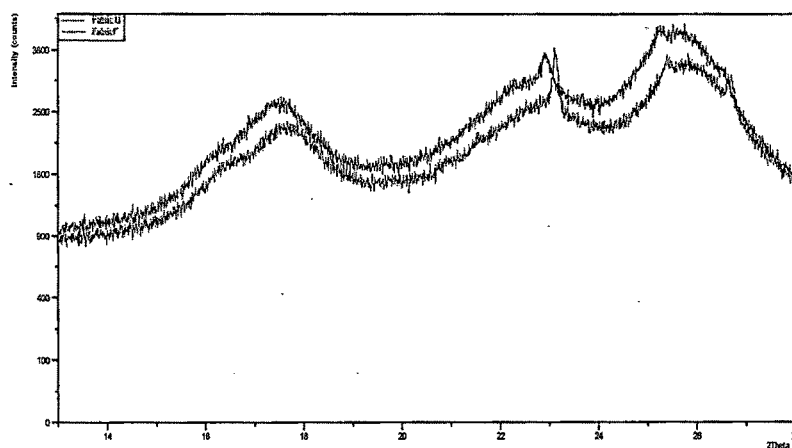


Figure 4.42 Combined XRD patterns of PT and NPT3 samples

4.3.1.4 Thermal analysis

Differential scanning calorimetry (DSC) was done to study the effect of incorporation of nano silica particles on thermal behavior of polyester fabric, which is shown in figure 4.43 and 4.44.

Table 4.15 Enthalpy (ΔH) of treated and untreated polyester fabric

| Sr. No. | Concentration of nano silica (g/l) | Melting Temperature $^{\circ}\text{C}$ | Enthalpy (ΔH) (J/g) |
|---------|------------------------------------|--|-------------------------------|
| 1 | 0.0 | 251.72 | 67.77 |
| 2 | 5.0 | 251.71 | 71.47 |

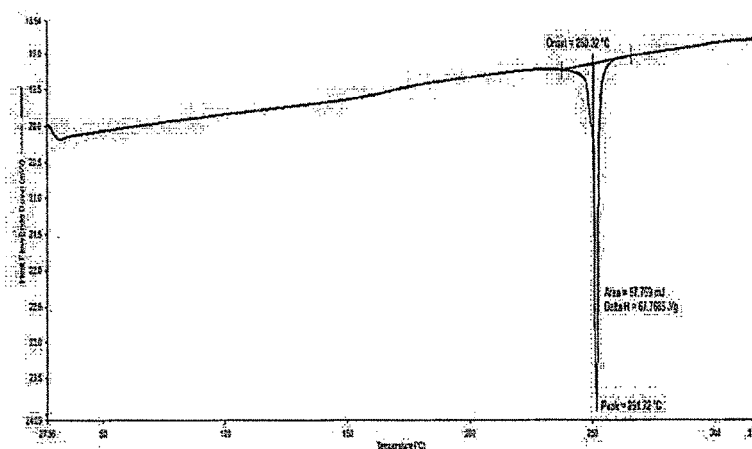


Figure 4.43 DSC curve of pure polyester fabric (PT)

Table 4.15 shows the melting temperature and enthalpy (ΔH) values of treated and untreated fabrics determined by DSC. Figure 4.43 shows the thermal behavior of pure polyester fabric. The melting temperature of polyester is 251.72°C and the enthalpy required to melt the pure polyester is 67.77 J/g . Figure 4.44 shows the thermal behavior of 5 gpl silica treated polyester silica nanocomposite fabric. The melting temperature of silica treated polyester fabric is 251.71°C , so there is no effect on melting temperature due to addition of silica nano particles. The enthalpy required to melt silica treated polyester fabric is 71.47 J/g . Due to nano silica treatment the rise in

enthalpy is by 5.46%. This rise in enthalpy may be due to nanoscopic level of silica, hence inducing better thermal stability to the fabric. Altan et. al [137] has made similar observation for polypropylene and polyester, being thermoplastic fibre may behave in the same manner due to the coating of nano SiO_2 particles. Similar observations are observed in earlier parts like in case of polyamide film and polypropylene filament, due to addition of silica nanoparticles the enthalpy required to melt the film/filament has also increased and there is no change in melting temperature due to addition of silica nanoparticles.

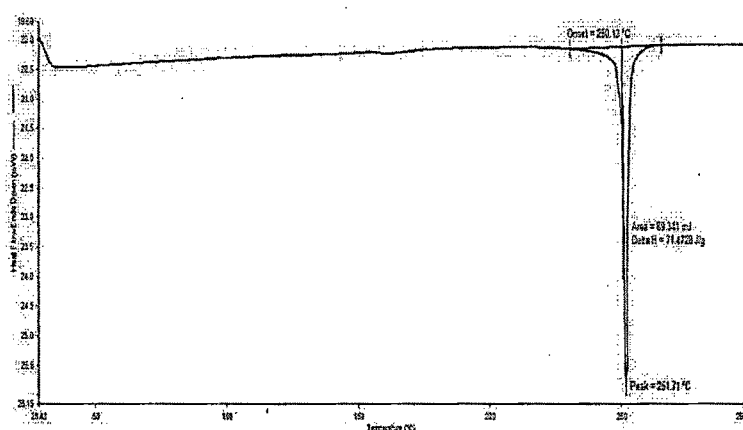


Figure 4.44 DSC curve of polyester fabric treated with 5gpl nano silica (NPT3)

4.3.2 MECHANICAL PROPERTIES

Treated and untreated polyester fabrics were evaluated for the change in their mechanical properties in terms of tensile strength, young's modulus, work of rupture, tearing strength and crease recovery angle. The treatment was carried out by pad-dry-cure method at different levels of concentration i.e. 1gpl, 2.5gpl and 5gpl of silica nano particles.

4.3.2.1 Tensile strength

Table 4.16 Tensile strength of polyester fabric

| Sample | Concentration of nano silica (g/l) | Tensile strength (Kgf) | | Stress Kgf/mm ² | | Strain % | |
|--------|------------------------------------|------------------------|-------|----------------------------|-------|----------|-------|
| | | Warp | Weft | Warp | Weft | Warp | Weft |
| | | way | way | way | way | way | way |
| PT | Untreated sample | 99.84 | 73.86 | 23.77 | 17.59 | 31.46 | 34.2 |
| NPT1 | 1.0 | 101.7 | 77.66 | 24.21 | 18.49 | 29.61 | 39.89 |
| NPT2 | 2.5 | 103.4 | 82.15 | 24.62 | 19.56 | 30.72 | 40.67 |
| NPT3 | 5.0 | 104.9 | 85.04 | 24.98 | 20.25 | 31.20 | 36.74 |

Gauge length = 200 mm, Thickness of fabric = 0.21 mm, Width of fabric = 20 mm, Cross sectional area = 4.2 mm²

The treated and untreated polyester samples were tested on Lloyd LRX tensile strength tester and the results are shown in table 4.16 and their tensile behavior is shown in figures 4.45 to 4.49. The untreated polyester fabric is showing 23.77 and 17.59 kgf/mm² stress in warp and weft way respectively. The stress value of warp direction is higher than the weft direction stress of polyester fabric. It may be due to the density of warp yarns is higher than the weft yarns i.e. 36 ends/cm, and 28 picks/cm respectively.

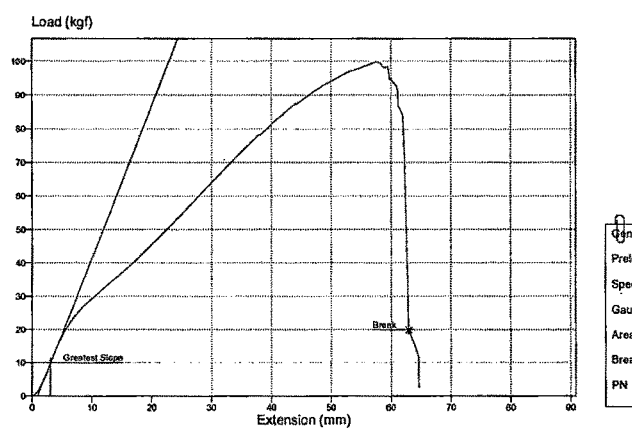


Figure 4.45 Load elongation behavior of pure polyester fabric (warp way)

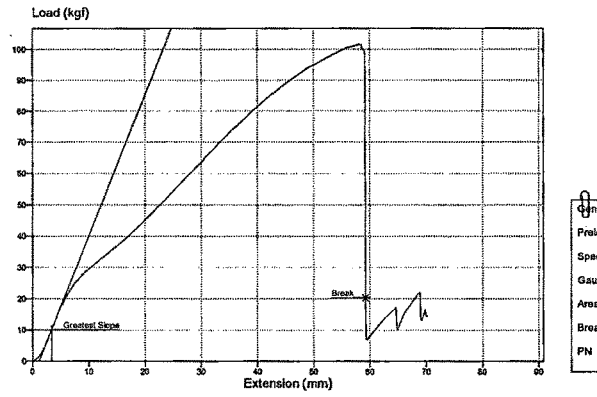


Figure 4.46 Load elongation behavior of 5 gpl polyester fabric (warp way)

Due to the treatment of nano silica in different concentrations to polyester fabric, the stress values in warp and weft direction are 24.21, 24.62 & 24.98 kgf/mm² and 18.49, 19.56 and 20.25 kgf/mm² respectively. The treatment of silica nano particles to the polyester fabric increases the stress property in warp as well as weft directions. This increase in strength may be due to binding caused by introduction of silica nano particles into the polymer matrix. The warp tensile strength is higher than the weft tensile strength because generally in warp, stronger yarns are used due to high stresses gets induced during weaving in the warp yarns as compare to the weft yarns and also the density of warp is higher than the weft yarns as explained above.

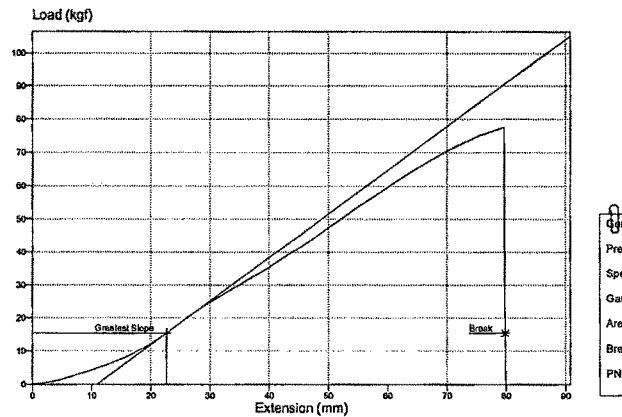


Figure 4.47 Load elongation behavior of pure polyester fabric (weft way)

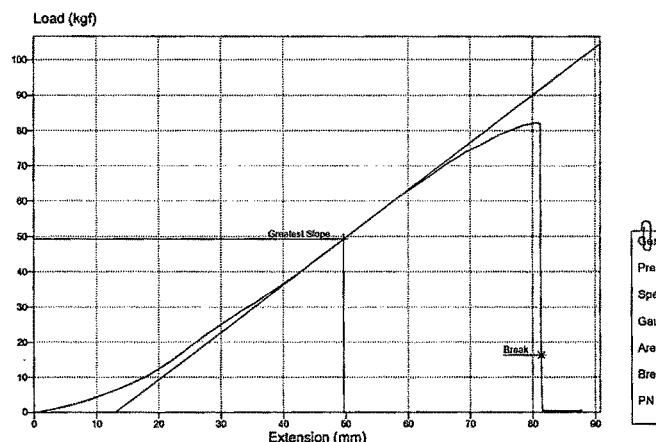


Figure 4.48 Load elongation behavior of 5 gpl polyester fabric (weft way)

The tensile strength is found increasing in both the directions as the concentration of silica nano particles increased. The percentage strain of warp and weft direction has not affected significantly due to the nano silica treatment. But the overall strain percentage of polyester fabric in weft direction is higher than the warp direction strain. This may be due to the less weaving tension in weft yarns during weaving, which may cause high crimp into the weft yarns.

The results are further supported by Mohltig et. al [22] 2005 reported that the possibility to increase the mechanical properties to be considered it as industrial nano reinforced fibre by treating the finished fabric with SiO_2 coating.

4.3.2.2 Young's modulus and work of rupture

The table 4.17 shows the young's modulus of untreated polyester fabric and nano silica treated polyester fabric. The young's modulus is calculated on the bases of Meredith's method. The untreated polyester fabric is showing 1.55 kgf/mm^2 young's modulus in warp direction and 0.44 kgf/mm^2 in weft direction. The warp direction young's modulus is higher than weft direction young's modulus, which means that the warp yarns are more stiffer than weft yarns, i.e. warp yarns can take more load with less deformation as compare to weft yarns. The young's modulus of nano silica treated polyester fabric in warp and weft directions is 1.51 , 1.53 and 1.57 kgf/mm^2 and 0.41 , 0.41 and 0.40 kgf/mm^2 respectively. Due to addition of nano silica particles

there is no significant change in young's modulus is observed in warp as well as weft direction. The young's modulus of polyester fabric in warp direction is higher than weft direction. The reason could be the same as given for the untreated polyester sample.

Table 4.17 Effect of nano silica on young's modulus and work of rupture of polyester fabric.

| Sample | Concentration of nano SiO ₂ (g/l) | Young's Modulus in (kgf/mm ²) | | Work of rupture at maximum load (kgf.mm) | |
|--------|--|---|------|--|----------|
| | | Warp | Weft | Warp way | Weft way |
| | | way | way | | |
| PT | 0.0 | 1.55 | 0.40 | 3475.3 | 2904.7 |
| NPT1 | 1 | 1.51 | 0.41 | 3748.6 | 3123.7 |
| NPT2 | 2.5 | 1.53 | 0.41 | 3853.1 | 3289.3 |
| NPT3 | 5 | 1.57 | 0.40 | 3997.8 | 3424.8 |

The "toughness" of the material is measured in terms of work of rupture of the material. The area under the load-elongation curve represents the work done in stretching the material to breaking point. The work of rupture value indicates the resistance of the material [148]. Table 4.17 shows the work at maximum load, of untreated polyester fabric and nano silica treated polyester fabrics. The work required to break the untreated polyester fabric (PT) is 3475.3 kgf.mm in warp direction and 2904.7 kgf.mm in weft direction. The work required to break the polyester fabric in warp direction is higher than the weft direction, which means that the warp direction polyester fabric is tougher than weft direction. As the work of rupture is a product of breaking load and elongation, the reason of high work of rupture in warp direction polyester fabric as compare to weft direction may be due to high breaking load required to break the polyester fabric in warp direction as compare to weft direction and the elongation at break of warp is less than weft direction polyester fabric but the difference in breaking load is much high as compare to the difference in elongation property of warp and weft direction polyester fabric.

The sample NPT1, NPT2 and NPT3 are showing increase in work of rupture to 3748.6, 3853.1 and 3997.8 kgf.mm in warp direction and 3123.7, 3289.3 and 3424.8 kgf.mm in weft direction as compare to PT sample, which means that to break treated samples high energy is required. The nano particles could be enhancing the work property of polyester fabric in both the directions. The work of rupture of polyester fabric in warp direction is higher than weft direction. The reason is same as above as higher breaking load required to break the polyester fabric in warp direction as compare to weft direction and the elongation at break of warp is less than weft direction polyester fabric but the difference in breaking load is much high as compare to the difference in elongation property of warp and weft direction polyester fabric.

4.3.2.3 Tearing strength

The treated and untreated samples were tested on Elmendorf tearing tester. Table 4.18 shows result of tearing strength of treated and untreated polyester fabric. Untreated polyester fabric tearing strength is 4352 and 3840 gf in warp and weft directions respectively. Here the warp direction tearing strength is higher than the weft direction tearing strength of polyester fabric. The reason could be high density of warp i.e. 36 ends/cm as compare to 28 picks/cm of weft. The treated samples, NPT1, NPT2 and NPT3 are showing minor improvement in tearing strength as compare to untreated sample. Also it is observed that as the concentration of silica nano particles increases, there is only 1 to 2 percentage increase in tearing strength, which is very minute. So, it can be interpreted that incorporation of nano silica particles does not affect the tearing strength of polyester fabric in both warp and weft direction. This may be due to the smaller size of the particle which may not be helping to improve tearing property.

Table 4.18 Tearing Strength of polyester fabric

| Sr. No. | Concentration of nano silica (g/lit) | Tearing Strength (gf) | |
|---------|---|-----------------------|----------|
| | | Warp way | Weft way |
| 1 | Untreated sample | 4352 | 3840 |
| 2 | 1 | 4388 | 3856 |
| 3 | 2.5 | 4412 | 3880 |

| | | | |
|---|---|------|------|
| 4 | 5 | 4458 | 3902 |
|---|---|------|------|

4.3.2.4 Crease recovery angle

The crease recovery test is a measure the ability of a fabric to resist creasing. The magnitude of this crease recovery angle is an indication of the ability of a fabric to recover from creasing [157].

Table 4.19 Crease Recovery Angle of Polyester fabric

| Sr. No | Concentration of nano silica (g/lt) | Warp way | | Weft way | |
|--------|-------------------------------------|----------|--------|----------|--------|
| | | 30 Sec | 60 Sec | 30 Sec | 60 Sec |
| 1 | Untreated sample | 140 | 147 | 105 | 110 |
| 2 | 1 | 142 | 147 | 109 | 114 |
| 3 | 2.5 | 145 | 148 | 110 | 116 |
| 4 | 5 | 147 | 151 | 113 | 119 |

The treated and untreated samples were tested on crease recovery angle tester and the results are shown in table 4.19. The crease recovery angle of untreated polyester fabric for warp way for 30 seconds and 60 seconds are 140° and 147° respectively. The weft way crease recovery angle for 30 seconds and 60 seconds are 105° and 110° respectively. The warp way crease recovery is higher than the weft way and as the time increases i.e. from 30 sec. to 60 sec. the recovery angle has increased in both the directions. Due to the treatment of silica nano particles in different concentrations as 1 gpl, 2.5 gpl and 5 gpl, the crease recovery angle has increased to 142, 145 & 147 and 147, 148 & 151 for 30 seconds and 60 seconds of warp way polyester fabric respectively. The weft way crease recovery angles are 109, 110 & 113 and 114, 116 & 119 for 30 seconds and 60 seconds respectively.

The result shows minor improvement in crease recovery angle of the treated samples i.e. warps way and weft way. The crease recovery angle is found increasing as the concentration of nano silica is increased. Overall the crease recovery angle in warp way is higher than the weft way in both treated and untreated samples. The silica nano particles because of their small size can enter in between the polymer molecules and perhaps act as filler or cross linking agent which also contributes to the load sharing phenomenon during load application to the material. Unlike chemical cross linking

which cause an improvement in crease recovery angle at the cost of imparting some rigidity in the material to an extent depending on the extent of cross linking. The incorporation of nano silica particle remains quite gentle in this regard. There was little improvement in the property which proves that the particles penetrated in between the polymer chain molecules, do not interfere much to the polymer flexibility. Also the crease recovery property of fabric improves with increase in the concentration of silica nano particles [158].